2014•2015
FACULTEIT GENEESKUNDE EN LEVENSWETENSCHAPPEN
master in de biomedische wetenschappen

Masterproef

Neuroprotective and neural reparative capacity of human dental pulp stem cells: identification of the CXCR4/SDF-1 migratory pathway

Promotor :
Prof. dr. Ivo LAMBRICHTS

Yörg Dillen
Scriptie ingediend tot het behalen van de graad van master in de biomedische wetenschappen

De transnationale Universiteit Limburg is een uniek samenwerkingsverband van twee universiteiten in twee landen: de Universiteit Hasselt en Maastricht University.

universiteit hasselt
KNOWLEDGE IN ACTION

Universiteit Hasselt | Campus Hasselt | Martelarenlaan 42 | BE-3500 Hasselt
Universiteit Hasselt | Campus Diepenbeek | Agoralaan Gebouw D | BE-3590 Diepenbeek

universiteit hasselt | Maastricht University

2014•2015
FACULTEIT GENEESKUNDE EN LEVENSWETENSCHAPPEN
master in de biomedische wetenschappen

Masterproef

Neuroprotective and neural reparative capacity of human dental pulp stem cells: identification of the CXCR4/SDF-1 migratory pathway

Promotor :
Prof. dr. Ivo LAMBRICHTS

Yörg Dillen
Scriptie ingediend tot het behalen van de graad van master in de biomedische wetenschappen

universiteit hasselt | Maastricht University

"If we knew what it was we were doing, it would not be called research, would it?"

Albert Einstein (1879 – 1955)

Acknowledgements

Ever since my bachelor years I was fascinated by the intriguing fields of neuroscience and stem cell biology. Therefore, I was excited that I could perform my senior internship on this project at the department of Morphology of Hasselt University. It has been a very instructive experience in which I could discover the real world of a biomedical researcher and the true value of a cup of coffee in the morning. Maybe the most important thing that I have learned during my internship is that in the field of research one cannot simply defy the law of Murphy. If it can go wrong, it surely will. However, with "discipline, dedication and friendship" every problem can be solved.

First of all, I would like to thank my promotor prof. dr. Ivo Lambrichts for giving me the opportunity to perform my internship in his research group. Few people have the gift of being successful and kind-hearted at the same time. You surely can count yourself amongst them.

I also would like to thank my daily supervisor Pascal Gervois for his advice and guidance during these eight months. His capacity to relativize is truly unmatched.

Furthermore, a word of gratitude for prof. dr. Tom Struys for his trust and guidance. I have no doubt he will be an excellent promotor during my PhD and I am privileged to be part of "Team Tom", the newest and coolest team of the Morphology department.

Also, many thanks for dr. Esther Wolfs, dr. Annelies Bronckaers, dr. Wendy Martens and dr. Evi Lemmens for their advice and critical feedback. Together with the other postdoctoral researchers, they are the driving force behind the science that is being conducted at the department of Morphology.

Thanks to Jessica Ratajczak and dr. Petra Hilkens for the amusing and instructive guidance and the support and advice during the writing of my FWO-project. Jessica, you definitely earned a sticker ;).

A word of appreciation goes out to Marc Jans and Jeanine Santermans for the help with the electron microscope and the immunostainings.

And of course, a big thank you for my fellow students or "BIOMED buddies". Cindy, Wim, Len, Hafida, Lauren, Ellen, Dorien, Joris and Jirka, you guys are awesome. I will never forget the funny moments we had at our little excursions and the weird discussions at the Friday afternoons. I wish you all the best of luck!

Finally, the most important thank you goes out to my family, in particular my mother, for the continuous support throughout my whole education.

Table of contents

List of abbreviations

BDNF Brain-derived neurotrophic factor

bFGF Basic fibroblast growth factor

BLBP Brain lipid-binding protein

BM-MNCs Bone marrow-derived mononuclear cells

BM-MSCs Bone marrow-derived mesenchymal stem cells

CM Conditioned medium

CNS Central nervous system

CXCR4 Chemokine receptor type 4

DAB Diaminobenzidine

DFPCs Dental follicle precursor cells

DMSO Dimethyl sulfoxide

EGF Epidermal growth factor

FBS Foetal bovine serum

FI Fluorescence intensity

GDNF Glial cell-derived neurotrophic factor

HBSS Hanks balanced salt solution

hDPSCs Human dental pulp stem cells

hESC Human embryonic stem cells

iPSCs Induced pluripotent stem cells

MEFs Mouse embryonic fibroblasts

MSCs Mesenchymal stem cells

NGF Nerve growth factor

NO Nitric oxide

NSCs Neural stem cells

NT-3 Neurotrophin-3

OGD Oxygen-glucose deprivation

PBS Phosphate buffered saline

pCNs Primary cortical neurons

PDGF-Rα Platelet-derived growth factor receptor alpha

PDLSCs Periodontal ligament stem cells

PFA Paraformaldehyde

ROS Reactive oxygen species

rtPA Recombinant tissue plasminogen activator

SCAP Stem cells from the apical papilla

SDF-1 Stromal cell-derived factor 1

SHED Stem cells from human exfoliated decidious teeth

TIMP1 Tissue inhibitor of metalloproteinase

tMCAO Transient middle cerebral artery occlusion

Tuj1 β3-tubulin

VEGF Vascular endothelial growth factor

α-MEM Alpha-modified minimum essential medium

Abstract

Introduction: Ischemic stroke is a severe condition which is defined by loss of brain function due to impaired blood flow to the brain. It is a major cause of permanent disability and is ranked as the second leading cause of death worldwide. Currently, there is no cure for stroke patients and existing treatment strategies are unable to sufficiently improve the functional outcome following stroke. However, cell-based therapy is considered a promising approach to minimize neurological damage and enhance functional recovery. In this study, the goal is to identify neuroprotective and neuroregenerative effects of human dental pulp stem cells (hDPSCs) *in vitro* and their potential underlying mechanisms.

Material & methods: The hDPSCs were isolated from extracted third molars with the explant method and were subsequently used for the production of conditioned medium. A neural stem cell (NSC) culture was established. Therefore, NSC were isolated from brains of mouse foetuses, cultured, morphologically analysed and phenotypically characterized by means of immunocytochemistry (ICC) and flow cytometry. Moreover, the CXCR4/SDF-1 migratory pathway was investigated in hDPSCs and NSCs with ICC. Furthermore, an oxygen-glucose deprivation (OGD) survival assay was developed. This required the establishment of a primary cortical neuron (pCN) culture. Consequently, the AlamarBlue® assay was validated in the pCN culture and the pCNs were subjected to varying OGD exposure times. Additionally, a H9 human embryonic stem cell (hESC) culture was introduced in the lab, which was morphologically and phenotypically analysed by means of transmission electron microscopy and ICC.

Results & discussion: A NSC culture with typical morphological characteristics was established and phenotypic analysis demonstrated that the isolated NSCs expressed a subset of the markers used for NSC characterization. However, it is recommended to perform additional characterization experiments to verify the purity of the acquired NSC culture. The obtained NSC culture can be used to evaluate the neuroregenerative capacity of hDPSCs *in vitro*. Furthermore, the CXCR4 chemokine receptor was identified in hDPSCs. The presence of the CXCR4 receptor could be of great importance for the homing of hDPSCs to the stroke lesion, since the CXCR4/SDF-1 axis has been described to play an important role in the migration of mesenchymal stem cells. Regarding the OGD survival assay, the use of a pCN density of at least 1.2×10^5 cells/cm^2 and an AlamarBlue® incubation time of 6h is suggested. Further research is necessary to determine the optimal OGD exposure time. Once the OGD survival assay is optimized, it can be assessed whether the secretome of hDPSCs is able to enhance survival of pCNs that are exposed to OGD. Additionally, a H9 hESC culture was established, which displayed morphological and phenotypic characteristics of a typical pluripotent stem cell culture.

Conclusion: The capacity of hDPSCs to exert neuroprotective and neuroregenerative effect *in vitro* could not be investigated yet. However, mandatory experiments were performed which were necessary to provide established cell cultures and knowledge about the optimal conditions for future assays. More elaborate research will grant information about the neuroprotective and neuroregenerative capacity of hDPSCs and reveal insight in the therapeutic potential of hDPSCs in ischaemic stroke.

Samenvatting

Inleiding: Een ischemisch herseninfarct is een ernstige aandoening die gedefinieerd kan worden door het verlies van hersenfunctie ten gevolge van een verstoorde bloedtoevoer naar de hersenen. Het is een van de meest prevalente oorzaken van permanente invaliditeit en is de op één na meest voorkomende doodsoorzaak wereldwijd. De bestaande therapeutische behandelingen zijn niet in staat om het functioneel herstel na een herseninfarct voldoende te verbeteren. Stamceltherapie wordt echter beschouwd als een veelbelovende strategie om de neurologische schade te minimaliseren en het functioneel herstel te bevorderen. Het doel van deze studie is om *in vitro* neuroprotectieve en neuroregeneratieve effecten van humane dentale pulpa stamcellen (hDPSC) te identificeren samen met hun mogelijke onderliggende mechanismen.

Materiaal & Methoden: De hDPSC werden geïsoleerd uit geëxtraheerde wijsheidstanden en vervolgens gebruikt voor de productie van geconditioneerd medium. Een neurale stamcel (NSC) cultuur werd tot stand gebracht. Hiervoor werden NSC geïsoleerd uit foetale muishersenen, in cultuur gebracht, morfologisch geanalyseerd en fenotypisch gekarakteriseerd door middel van immunocytochemie (ICC) en flowcytometrie. Verder, werd de CXCR4/SDF-1 migratie as onderzocht in hDPSC en NSC met behulp van ICC. In deze studie werd ook een zuurstof-glucose deprivatie (OGD) assay ontwikkeld. Hiervoor moest echter een cultuur van primaire corticale neuronen (pCN) opgestart worden. Vervolgens, werd de AlamarBlue® assay gevalideerd voor het gebruik bij pCN culturen en werden de pCN blootgesteld aan verschillende periodes van OGD. Bijkomend, werd een cultuur van H9 humane embryonale stamcellen (hESC) opgestart en werd deze morfologisch en fenotypisch geanalyseerd met behulp van transmissie elektronen microscopie en ICC.

Resultaten & Discussie: Een cultuur met typische morfologische kenmerken van NSC werd tot stand gebracht. Fenotypische analyse toonde aan dat deze cellen de voornaamste merkers voor de identificatie van NSC tot expressie brachten. Het wordt echter aangeraden om verdere karakterisatie uit te voeren om de zuiverheid van de cultuur te verifiëren. De NSC cultuur kan gebruikt worden om de neuroregeneratieve capaciteit van de hDPSC te onderzoeken. Verder, werd de CXCR4 receptor geïdentificeerd in hDPSC. De expressie van deze receptor kan van groot belang zijn voor de migratie van hDPSC naar de ischemische laesie, vermits de CXCR4/SDF-1 as een belangrijke rol speelt bij de migratie van mesenchymale stamcellen. Aangaande de OGD assay, wordt het aangeraden om een densiteit van tenminste 1.2×10^5 cellen/cm^2 en een AlamarBlue® incubatietijd van 6u te gebruiken. Verder onderzoek is nodig om de optimale OGD tijd te bepalen. Eens geoptimaliseerd, kan de OGD assay gebruikt worden om te onderzoeken of de hDPSC de overleving van OGD beschadigde pCN verhoogt. Bijkomend, werd een H9 hESC cultuur opgestart die de morfologische en fenotypische karakteristieken van een typische pluripotente stamcelcultuur vertoonde.

Conclusie: De capaciteit van hDPSC om neuroprotectieve en neuroregeneratieve effecten uit te voeren kon nog niet onderzocht worden. De basis hiervan werd echter gelegd door het uitvoeren van essentiële experimenten waardoor de nodige celculturen werden voorzien en belangrijke informatie werd verkrijgen omtrent de optimale condities voor de toekomstige assays. Verder onderzoek is vereist om de neuroprotectieve en neuroregeneratieve capaciteit van hDPSCs te verduidelijken en daarbij inzicht te verwerven in het therapeutisch potentieel van de hDPSC bij patiënten met een ischemisch herseninfarct.

1 Introduction

Ischaemic stroke is a severe condition which is defined by loss of brain function due to impaired blood flow to the affected area in the brain. It is a major cause of permanent disability and is ranked as the second leading cause of death worldwide [1]. The incidence of stroke ranges from 240 to 600 per 100,000 people and in developed countries more than 4% of direct healthcare costs is consumed for stroke management [2]. Since the highest incidence is seen in people older than 65, the social and economic burden caused by stroke keeps on rising, given the ageing of the population. Severe neurological damage can be observed following stroke. Clinically this is translated into disabilities such as paralysis, sensory disturbances, aphasia, memory loss, urinary incontinence, cognitive impairment and emotional instability, depending on the affected area of the brain. Ischaemic stroke is the most common type, covering about 80% of all stroke cases. The five most prevalent causes of ischaemic stroke are thrombosis, embolism, systemic hypoperfusion, arterial luminal obliteration and venous congestion. The brain is particularly vulnerable to ischaemia-induced damage, due to its high oxygen-dependent glucose consumption, limited glucose storage capacity and high levels of substrates for reactive oxygen species (ROS) [3].

1.1 Pathophysiology of ischaemic stroke

During ischaemic stroke, a disturbed blood supply leads to oxygen and glucose deprivation in the affected area. This triggers a complex cascade of biochemical events which result in the induction of neuronal cell death. Ischaemia causes energy failure, since the brain depends almost exclusively on oxygen and glucose provision for the production of adenosine triphosphate (ATP) [4]. Consequently, the ionic homeostasis is disrupted (i.e. aberrant concentrations of ionised sodium, potassium and calcium), leading to excessive glutamate release via membrane depolarization, mitochondrial failure, acidosis, ROS accumulation, activation of proteolytic enzymes and nitric oxide (NO) production [5]. The high amounts of glutamate in the extracellular space overstimulate N-methyl-d-aspartate (NMDA) receptors and α-amino-3-hydroxy-5-methyl-4-proprionate (AMPA) receptors, resulting in additional calcium influx and NO production. Mitochondrial failure and disruption leads to a burst in free radicals and release of proapoptotic molecules such as cytochrome C [6]. NO and ROS disrupt the integrity of cellular components and damage DNA. Via various molecular pathways, all these deleterious events promote the induction of cell death. Three zones can be distinguished in the acute stroke lesion. The core is defined by having a perfusion of less than 12 ml/100g/min and the neuronal cells in this zone predominantly undergo necrosis. The penumbra, surrounding the core, is critically hypoperfused (approximately 35 ml/100g/min or less) and will progress into infarction without reperfusion. Neuronal cells in this zone are dysfunctional and gradually undergo apoptosis if left untreated. The benign oligemia is the most peripheral zone of the acute lesion and will spontaneously recover over time [7].

The pathophysiologic cascade also causes oedema formation [8]. Cytotoxic oedema develops within minutes to hours after the ischaemic insult due to energy failure and ionic imbalance. The influx of sodium mediates intracellular water accumulation, which can result in osmotic lysis of the cell. Additionally, formation of vasogenic oedema is initiated within hours to days, due to disruption of

the blood-brain barrier. This is characterized by high amounts of fluid in the extracellular space, putting increasing pressure on the brain.

Besides the direct pathophysiologic processes which cause neuronal cell death, a strong immune response is provoked by the secretion of proinflammatory cytokines (i.e. IL-1β, IL-6 and TNF-α), chemokines (i.e. MCP-1, chemokine ligand 1) and matrix metalloproteases [9]. Subsequently, immune cells are attracted and infiltrate the lesion, resulting in additional neuronal cell death and scar formation [10].

1.2 Current treatment of ischaemic stroke and novel approaches

Currently, recanalization of the obstructed blood vessel with recombinant tissue plasminogen activator (rtPA) is the only specific pharmacological treatment for ischaemic stroke, which is approved by the US Food and Drug Administration (FDA) [11]. The goal of recanalization is to remove the obstruction to allow reperfusion of the ischaemic area. However, rtPA treatment is far from ideal since it needs to be administered within 4 to 5 hours after the ischaemic onset, thereby limiting its use to only 2-4% of the patients [12]. Furthermore, initiation of the treatment after the therapeutic time window is associated with an increased mortality [13]. Alternative mechanical recanalization techniques, including stenting and thrombectomy devices, are available. However, they do not provide a superior outcome to rtPA treatment, leaving rtPA treatment the standard therapy of ischaemic stroke [14].

There is an urgent medical need for improved therapeutic options, since modern medicine is unable to provide adequate therapy for stroke patients. Therefore, current research aims to develop novel strategies beyond recanalization to improve the functional outcome in stroke patients. In general, two approaches are distinguished: the neuroprotective approach and the neuroregenerative approach.

Any strategy that aims to inhibit or antagonize the pathophysiological cascade of biochemical events which result in irreversible cell damage and eventually neuronal cell death is considered a neuroprotective approach [15]. Neurons located in the ischaemic core die within minutes after stroke onset, whereas peripheral neurons located in the penumbra, provided with collateral blood flow, become dysfunctional but do not undergo acute cell death. Due to secondary damage from excitotoxicity and chronic inflammation, the penumbra may progress into infarction via delayed neuronal cell death hours to days after the ischaemic insult [16]. Therefore, a time window exists wherein reversibly damaged neurons can be salvaged from cell death and thereby limit infarct size and improve functional outcome after stroke. Various neuroprotective agents which target different components of the pathophysiological cascade have been investigated in the context of stroke (reviewed by Moretti et al., 2015) [11]. Despite promising preclinical results, no neuroprotective agent has passed the clinical trials. Nonetheless, the concept of neuroprotection remains a field of intense research.

The neuroregenerative approach aims to improve the functional outcome in stroke patients by enhancing endogenous repair mechanisms. Following stroke, endogenous repair mechanisms including neurogenesis, angiogenesis, neurite outgrowth and synaptogenesis are activated [17, 18].

However, these endogenous mechanisms are not potent enough to acquire adequate functional recovery in stroke patients. Therefore, stimulation of endogenous repair mechanisms in stroke patients could allow the brain to compensate the neuronal damage and restore the neurological function. Various pharmacological agents including statins, minocycline and nicotinic acid, as well as stem-cell-based strategies are under investigation in the hope to develop a therapy that is able to sufficiently improve the functional outcome in stroke patients.

1.3 Stem cells

A stem cell is defined by having the capacity of unlimited self-renewal as well as the ability to terminally differentiate into one or more cell types. This implies that the cell undergoes symmetric replication, resulting in the formation of two identical daughter cells, in order to sustain the stem cell pool, while it can also undergo committed differentiation to provide specialized mature cells for the generation of tissue. Based on their potency, stem cells can be divided into different subtypes. Totipotent stem cells are the stem cells with the highest differentiation potential and can only be found in the morula, the first stage of embryogenesis. They can differentiate into both embryonic and extraembryonic cell types and thereby are able to create a complete, viable organism. Pluripotent stem cells are derived from the inner cell mass of an early blastocyst and can differentiate into every cell types of the three germ layers. Stem cells are not only present in the embryonic and foetal stages, but also in the postnatal human body. These stem cells are termed postnatal stem cells and reside in various tissues. They are responsible for the natural turn-over of tissue and in case of tissue damage can contribute to regeneration of the lost tissue. Amongst the postnatal stem cells a discrimination can be made between multipotent stem cells, which are able to differentiate into several cell types derived from one germ layer, and unipotent stem cells, which can only differentiate into one specific cell type [19].

1.3.1 Human dental pulp stem cells

Depending on their location in the body and differentiation potential, several postnatal stem cell types can be distinguished (e.g. neural stem cells, hematopoietic stem cells and mesenchymal stem cells). Mesenchymal stem cells (MSCs) are by far the most extensively investigated type of stem cells. They can be found in various tissues including bone marrow, umbilical cord, adipose tissue, the placenta and dental tissue [20]. Accurate identification of MSCs remains a challenge, since a single specific marker is lacking. Therefore, cells have to meet the following three criteria to be considered MSCs: (1) plastic adherence, (2) expression of a panel of markers and (3) multipotent trilineage differentiation capacity *in vitro* (towards osteocytes, chondrocytes and adipocytes). By definition of the International Society for Cellular Therapy (ISCT), MSCs should express CD73, CD90 and CD105 and lack expression of CD11b, CD14, CD19, CD34, CD45, CD79α and HLA-DR [21]. Mesenchymal SCs have a high expansion potential, are able to migrate towards the site of injury and have immunosuppressive properties. Therefore, they hold great promise for the development of stem cell-based therapy in various pathological conditions, including cardiovascular disease, neurological diseases and even inherited diseases [22, 23].

A relatively new source of mesenchymal stem cells are dental stem cells. In 2000, the group of Gronthos discovered the presence of a stem cell population in human dental pulp, termed human

dental pulp stem cells (hDPSCs) [24]. In the following years, other dental stem cell populations have been identified: stem cells from human exfoliated deciduous teeth (SHED), periodontal ligament stem cells (PDLSCs), stem cells from the apical papilla (SCAP) and dental follicle precursor cells (DFPCs) [25-28]. These types of dental stem cells residing in different tissues of the oral and maxillofacial area, are derived from different stages of tooth development and each type has specific characteristics and advantages (reviewed by Martens et al., 2013) [20].

Human DPSCs are a clonogenic, heterogeneous stem cell population with high proliferation capacity and multi-lineage differentiation potential [29]. They derive from neural crest cells and therefore are considered ectomesenchymal-derived stem cells. Furthermore, hDPSCs have a fibroblast-like morphology, adhere to plastic in culture and have a similar expression pattern of mesenchymal markers compared to bone marrow-derived mesenchymal stem cells (BM-MSCs). They express CD29, CD44, CD59, CD73, CD90, CD105, CD106 and CD146 and lack expression of hematopoietic markers CD11b, CD34, CD45 [30, 31]. Moreover, hDPSCs are able to differentiate into osteogenic, chondrogenic, adipogenic, odontogenic, melanogenic and neurogenic cell types *in vitro* [29, 32-34]. Initially, research regarding hDPSCs was mainly focused on the development of applications for tooth regeneration and dental tissue repair, since they can produce dentin-pulp-like tissue and dentin-like structures *in vivo* [24, 35]. However, several studies also indicate the potential use of hDPSCs in other clinical domains. For example, hDPSCs are able to enhance angiogenesis in rodent models of myocardial infarction and hind limb ischaemia and to promote neurogenesis and functional recovery in rodent models of stroke and spinal cord injury, thereby providing evidence for their potential use in various pathological conditions [36-39]. Also, the ability of hDPSCs to express neural markers, secrete neurotrophic factors, differentiate into neurons and induce axon guidance suggests a potential role in cell-based therapy of neurological diseases [33, 40, 41]. Additionally, it has been demonstrated that hDPSCs retain their stem cell properties and differentiation potential after long-term cryopreservation, making them suitable for stem cell banking and clinical use [42].

1.3.2 Pluripotent stem cells

The research group of Thomson was the first to generate human embryonic stem cells (hESCs) which comply with the three essential criteria of an embryonic stem cell, namely (1) derivation from the pre-implantation embryo, (2) sustained undifferentiated proliferation and (3) the potential to generate derivatives of the three germ layers [43]. This scientific breakthrough provided new opportunities, since hESCs are a useful tool for studying human developmental biology and can have applications in drug discovery and regenerative medicine. Various hESC lines with a stable karyotype, high telomerase activity and expression of pluripotency markers, like stage-specific embryonic antigen (SSEA)-3, SSEA-4, teratocarcinoma recognition antigen (Tra)-1-60, Tra-1-81, oct-4 and Nanog, have been established [44]. The hESC lines are considered the golden standard of pluripotent stem cells. However, ethical controversy has been a major hurdle in exploiting the translational value of pluripotent stem cells.

In 2006, Takahashi and Yamanaka demonstrated that the introduction of c-myc, oct3/4, sox2 and klf4, four key transcription factor genes, in adult mouse fibroblasts resulted in the formation of cells with embryonic-like features [45]. This discovery revealed that mature somatic cells can also be reprogrammed to the embryonic state, a process termed induced pluripotency. Subsequently,

further elaboration on these findings resulted in successful induction of pluripotency in human fibroblasts, designating with the term induced pluripotent stem cells (iPSCs) [46]. Other research groups have improved the protocol to exclude the use of the oncogenic c-myc gene and even exclude the use of retroviral transfection [47, 48]. The iPSCs show great similarity with hESCs and do not require the sacrifice of human embryos, thereby circumventing major ethical concerns. The development of iPSCs has revitalized the field of pluripotent stem cell research and provided new opportunities.

Progress is being made towards using iPSC in regenerative medicine. For example, transplantation of iPSC-derived dopaminergic neurons in different animal models of Parkinson's disease showed integration in the midbrain, long-term survival and an improved functional outcome [49]. Furthermore, iPSC-derived neurospheres which were grafted in a mouse model of spinal cord injury demonstrated to migrate towards the lesion, differentiate into neurons, astrocytes and oligodendrocytes *in vivo* and improve motor function [50]. Other studies also showed beneficial effects of iPSC-derived cells in animal models of stroke [51, 52]. Besides exploring the potential of iPSC in therapeutic strategies, iPSCs are also employed for disease modelling and drug screening. Patient-derived iPSCs are being utilized to recapitulate the disease phenotype *in vitro* and investigate the fundamental pathophysiological mechanisms of the disease of interest. This 'patient-in-a-dish' concept has proven itself to be useful, even in polygenic diseases like Parkinson's disease, Alzheimer's disease and schizophrenia [53-55]. Consequently, this provides a novel tool to screen more accurately for candidate drugs for the treatment of the disease of interest, thereby improving the extensive process of drug development.

1.4 Stem cell therapy in ischaemic stroke

As mentioned previously, endogenous neural repair is limited and current treatment strategies are unable to sufficiently improve the functional outcome after stroke. However, stem-cell-based therapy is considered a promising approach to minimize neurological damage and enhance functional recovery following stroke. Several preclinical studies comprising various cell types show beneficial effects on the functional outcome in animal models of stroke [56]. Furthermore, a systematic review of the first clinical trials in stroke patients suggests stem cell therapy to be safe and feasible [57]. However, translation to an effective therapy is facing various difficulties, including the identification of the optimal stem cell source, amount of cells to use, administration route and therapeutic window. Currently, only limited knowledge is available about the mechanisms of action used by stem cells to mediate neural repair. Therefore, elucidating the mechanisms of action used in neural repair will aid in overcoming these difficulties in the development of an effective cell-based therapy for stroke patients.

1.4.1 Human DPSCs and iPSCs are promising candidates for stem cell therapy in stroke

In order to develop an effective cell-based therapy for stroke, it is essential to exploit the optimal stem cell source. The first clinical trials used mainly BM-MSCs and bone marrow-derived mononuclear cells (BM-MNCs). However, in search for the optimal stem cell source, hDPSCs and iPSCs seem to hold greater promise. Like bone marrow stem cells, hDPSCs and iPSCs can be used

autologous. Though, hDPSCs and somatic cells for the generation of iPSCs can be isolated with lower donor site morbidity, thereby circumventing the complications related to BM-MSC isolation [58].

Furthermore, hDPSCs have a rich secretome including brain-derived neurotrophic factor (BDNF), nerve growth factor (NGF), neurotrophin-3 (NT-3) and glial cell-derived neurotrophic factor (GDNF), which are considered important neurotrophic and neuroregulatory factors. A recent study showed that the secretion of BDNF, NGF and NT-3 is significantly higher in hDPSCs compared to BM-MSCs [59]. In addition, the research group of *Song et al.* demonstrated hDPSCs to exert superior cytoprotection against cell death in ischaemic human astrocytes compared with BM-MSCs [60]. Previous secretome based studies performed in our lab also showed enhanced neurite outgrowth in SH-SY5Y neuroblastoma cells after exposure to the conditioned medium of hDPSCs, indicating a potential role of hDPSCs in stimulating endogenous neurogenesis. Regarding the secretome of iPSCs, less information is available. A limited analysis of the secretome of rat iPSCs revealed secretion of vascular endothelial growth factor (VEGF) and tissue inhibitor of metalloproteinases 1 (TIMP1) [61]. However, more extensive analysis of the iPSCs secretome is required to provide a more detailed picture of the secretory profile of iPSCs. Additionally, the capacity of hDPSCs and iPSCs to differentiate into neurons with functional characteristics and integrate in the brain circuitry following transplantation is an essential feature regarding cell replacement approaches [33, 62, 63].

In vivo studies with DPSCs and iPSCs already have demonstrated to exert beneficial effects following transplantation in rodent stroke models. Enhanced functional recovery has been observed after transplantation of hDPSCs in the transient middle cerebral artery occlusion (tMCAO) model of stroke and injection of hDPSCs in rats with ischaemic brain damage has shown to ameliorate behavioural dysfunction and lesion severity [38, 64]. Furthermore, two independent research groups demonstrated human iPSC-derived neurons to promote functional recovery after transplantation in stroke-damaged rats [51, 52]. Taken together, hDPSCs and iPSCs are proposed as promising candidates for future cell-based therapy in stroke patients.

1.4.2 Potential beneficial mechanisms of action of hDPSCs and iPSCs in stroke

Following stem cell transplantation, both paracrine effects and cell replacement can be responsible for improved functional outcome after stroke. In the concept of cell replacement, the transplanted stem cells need to migrate towards the lesion, differentiate into neurons and integrate with the local circuitry to enable functional recovery. Initially, cell replacement was believed to be the main mechanism of action in cell-based therapy. However, increasing evidence suggests that the paracrine factors secreted by the stem cells play a prominent role in ameliorating disease outcome. Transplanted hDPSCs have been shown to use secretome-mediated mechanisms, including neuroprotection, neuroregeneration, immuno-regulation and stimulation of neovascularization to improve disease outcome, as already demonstrated in spinal cord injury and other diseases [36, 39, 65-67]. Regarding iPSCs, less information is available about the paracrine effects *in vivo* since iPSCs tend to form teratomas after transplantation and thus are rarely used for cell-based therapy as such. Therefore, iPSCs are often pre-differentiated towards more dedicated cell types prior to transplantation. Depending on the disease, different cell types can be of interest which all have their specific secretome and consequently their distinct paracrine effects.

1.5 Research aims and experimental setup

The goal of this study is to identify neuroprotective and neuroregenerative effects of hDPSCs and their potential underlying mechanisms. Providing stressed neurons with neurotrophic and anti-apoptotic signals could allow them to survive the harsh conditions in the acute phase of stroke, thereby limiting stroke severity and neurological damage. Furthermore, stimulating neuroregeneration after stroke could result in enhanced functional recovery. Investigating both the short- and long-term beneficial effects of hDPSCs on the disease outcome in stroke is essential for a profound understanding of the therapeutic potential.

Following transplantation, hDPSCs have to be able to migrate towards the site of injury to mediate their paracrine effects. The CXCR4/SDF-1 migratory pathway will be investigated in the context of stroke. The expression of the transmembrane C-X-C chemokine receptor type 4 (CXCR4) on the surface of hDPSCs will be examined using immunocytochemical analysis. Moreover, the production of SDF-1 by hDPSCs and the expression of CXCR4 in mouse neural stem cells (NSCs) will be investigated. Therefore, a NSC culture needs to be established. This requires isolation of NSCs from foetal mice, followed by prolonged culture. The NSC culture will be characterized by assessing the expression of stem cell markers using flow cytometry and immunocytochemical staining. To evaluate the neuroprotective capacity of hDPSCs *in vitro*, an oxygen-glucose deprivation (OGD) survival assay will be developed. Therefore, primary cortical neurons (pCNs) are isolated from foetal mice and cultured. The optimal cell density for culture of pCNs will be determined. Cell viability and cell death will be the outcome values for the OGD survival assay. To measure these outcome values, optimization of the AlamarBlue® viability assay and the flow cytometric Annexin V/PI apoptosis assay will be performed. Furthermore, the effect of the conditioned medium of hDPSCs on neurite outgrowth in pCNs will be investigated.

Additionally, the therapeutic potential of iPSCs in stroke is also of great interest. In order to investigate these pluripotent stem cells in our lab, an iPSC culture has to be established. Prior to introducing an iPSC culture in the lab, we commence culturing H9 hESCs. The H9 hESC culture will be morphologically and ultrastructural analysed in addition to evaluating the expression of hallmark pluripotency markers. The culture of these H9 hESCs is essential to gain experience in culturing pluripotent stem cells and allows comparison of the introduced iPSC culture with an already established culture of pluripotent stem cells.

2 Materials and methods

A detailed overview of the experimental procedures including cell culture, optimization of an oxygen-glucose deprivation survival assay, flow cytometry, transmission electron microscopy and immunocytochemistry is provided in the following sections.

2.1 Isolation and culture of human dental pulp stem cells

The hDPSCs were isolated from third molars by means of an explant culture. Third molars which were extracted for aesthetic or therapeutic reasons were obtained from Ziekenhuis Oost-Limburg with informed consent of the donor or guardian and after approval by the ethical committee of Hasselt University (13/0104U). Average age of the donors was 17.7 years (SD = 2.2). After extraction, third molars were mechanically fractured to reveal the central pulp cavity, containing the dental pulp tissue. Apical papilla tissue was carefully removed and the isolated dental pulp tissue was put in pre-warmed alpha-modified Minimum Essential Medium (α-MEM) (Sigma, St. Louis, United states of America) supplemented with 10% foetal bovine serum (FBS) (Gibco, Paisley, United Kingdom), 2 mM L-glutamine (Sigma), 100 U/ml penicillin and 100 µg/ml streptomycin (Sigma) (referred to as standard hDPSC medium). Subsequently, the dental pulp tissue was fragmentised and cultured in 6-well plates (Greiner Bio-one, Wemmel, Belgium) to allow adherence an hDPSC outgrowth (37°C, 5% CO_2). The culture medium was changed every 3-4 days and the explant culture was evaluated by means of a phase contrast microscope (Nikon Eclipse TS100, Japan). Human DPSCs were sub-cultured when 70-80% confluence was reached. Therefore, hDPSCs were harvested by incubation with 0.05% trypsin/EDTA (Sigma) for 5-10 min (37°C, 5% CO_2). Thereafter, the cell suspension was centrifuged (Eppendorf 5804R, Rotselaar, Belgium) at 300g for 6 min. Cell counting was performed using a Fuchs Rosenthal counting chamber after staining with trypan blue solution (Sigma). Cells were seeded at a density of 4 x 10^3 cells/cm^2 in T25 or T75 culture flasks (Greiner Bio-one) and the medium was changed every 3-4 days. Human DPSCs were cryopreserved at -80°C in α-MEM supplemented with 20% FBS and 10% Dimethyl sulfoxide (DMSO, Sigma). Temperature was gradually reduced at a rate of 1°C per min, using a CoolCell (BioCision, San Rafael, United States of America). For immunocytochemical analysis, hDPSCs were seeded at a density of 5 x 10^3 cells/cm^2. Cells from passage 1 to 10 were used to perform experiments.

2.2 Production of conditioned medium

For the production of conditioned medium (CM), hDPSCs were seeded at a density of 2 x 10^4 cells/cm^2 in standard culture medium. 24h later, the cells were rinsed with phosphate buffered saline (PBS) and cultured in appropriate medium at a concentration of 1 x 10^5 cells/ml. The media used for the production of CM were standard hDPSC medium supplemented with 0.1% FBS, standard pCN medium and Neurobasal A medium supplemented with 2 mM L-glutamine, 0.1% N-2 supplement (Invitrogen), 100 U/ml penicillin and 100 µg/ml streptomycin, After 48h, the conditioned medium was collected and centrifuged at 300g for 6 min to pellet cell debris. Finally, the supernatant was stored at -80°C.

2.3 Isolation and culture of mouse cortical neurons

Primary cortical neurons (pCNs) were isolated from mouse foetuses (C57Bl/6) at gestational days 17-18 as approved by the ethical committee (protocol number 201410). Therefore, a pregnant mouse was sacrificed by means of cervical dislocation and foetuses were collected. The brains of the foetuses were isolated and kept in Hank's balanced salt solution (HBSS) supplemented with 7 mM hepes, 100 U/ml penicillin and 100 µg/ml streptomycin (all from Invitrogen). Using a Leica S6E stereo microscope (Leica microsystems, Wetzlar, Germany), the meninges were removed from the brain and the cortices were collected in supplemented HBSS. The cortices were incubated with 0.05% trypsin/EDTA solution (Invitrogen) for 15 min (37°C) and washed three times in Minimum Essential Medium (MEM) (Invitrogen) supplemented with 10% horse serum (Gibco), 0.6% glucose, 100 U/ml penicillin and 100 µg/ml streptomycin. Thereafter, the cortices were mechanically dissociated by pipetting up and down for about 30 times with a glass Pasteur pipet with decreasing diameter. The acquired cell suspension was centrifuged for 8 min at 300g (12°C). Then, the cells were resuspended in supplemented MEM medium and rinsed through a 70 µM cell strainer (Thermo Fisher Scientific, Erembodegem, Belgium). Neurons were seeded at varying densities in culture plates coated with 20 µg/ml poly-d-lysine (Corning). When the neurons were attached to the coated surface of the plates, the medium was changed to neurobasal medium supplemented with 2 mM L-glutamine, 2% serum-free B27, 100 U/ml penicillin and 100 µg/ml streptomycin (all from Invitrogen) (referred to as standard pCN medium). Neurons were cultured for up to two weeks, without medium change (37°C, 5% CO_2). For immunocytochemical analysis, the pCNs were seeded at a density of 1.8 x 10^4 cells/cm^2.

2.4 Induction of oxygen-glucose deprivation and glutamate excitotoxicity

Prior to the induction of oxygen-glucose deprivation (OGD) and glutamate excitotoxicity, the pCNs were seeded at a density of 6 x 10^4 cells/cm^2 in 96-well plates (Greiner Bio-one) and cultured in standard pCN medium for five days to allow maturation of the neurons. Consequently, the cells were exposed to OGD or glutamate excitotoxicity. Therefore, the medium was disposed and the cells were washed with PBS. To induce OGD, cells were incubated in DMEM without glucose (Invitrogen) and placed inside a BD GasPak EZ anaerobe gas generating pouch system (BD, Erembodegem, Belgium) for 1h, 3h and 24h (37°C, 0% O_2, 5-10% CO_2). To induce glutamate excitotoxicity, cells were incubated in standard pCN medium supplemented with varying concentrations (250 µM to 8 mM) of L-glutamic acid (Sigma) for 1h, 3h and 24h (37°C, 5% CO_2). After exposure to OGD or glutamate excitotoxicity, the cells were washed with PBS and incubated with the appropriate medium for up to 24h (37°C, 5% CO_2). Cell viability or cell death were evaluated as described in the following sections.

2.4.1 Evaluation of cell viability with the AlamarBlue® viability assay

Cell health was evaluated by means of the AlamarBlue® viability assay. The AlamarBlue® dye (Invitrogen) was added to the medium (10% of volume) and incubated for 6h (37°C, 5% CO_2). Thereafter, the fluorescence intensity (FI) at 590 nm was measured using a FLUOstar omega microplate reader (BMG Labtech, Temse, Belgium) with excitation at 540 nm. Each experiment was performed in triplicate.

2.4.2 Evaluation of cell death with the annexin V and propidium iodide apoptosis assay

Cell death was evaluated by means of the Annexin V-FITC Apoptosis Detection Kit (eBioscience, Vienna, Austria), according to the manufacturers protocol. Briefly, the pCNs were harvested by incubation with 0.05% trypsin/EDTA for 15 min (37°C, 5% CO_2) and transferred to a V-bottom 96-well plate (Greiner Bio-one). Subsequently, the cells were centrifuged at 600g for 5 min and resuspended in binding buffer (BD). Next, FITC-conjugated annexin V was added at a dilution of 1/20 and the cells were incubated for 15 min at room temperature. Thereafter, cells were washed with binding buffer and resuspended in binding buffer supplemented with propidium iodide staining solution at a dilution of 1/40. Analysis was performed by means the BD FACSCalibur System (BD), using BD CellQuest Pro Software.

2.5 Isolation and culture of mouse neural stem cells

Neural stem cells (NSCs) were isolated from mouse embryos (C57Bl/6) at gestational days 13-15 as approved by the ethical committee (protocol number 201410). Therefore, a pregnant mouse was sacrificed by means of cervical dislocation and the foetuses were collected. The brains of the foetuses were isolated and kept in cold PBS supplemented with 100 U/ml penicillin and 100 µg/ml streptomycin. Then, the brains were cut into small fragments and centrifuged for 8 min at 200g. The brain fragments were resuspended in PBS supplemented with 2 mg/ml collagenase A (Roche, Vilvoorde, Belgium) and 10 µg/ml deoxyribonuclease I (Sigma) and incubated for 90 min (37°C, 5% CO_2). Thereafter, the fragments were centrifuged for 5 min at 300g and resuspended in neurobasal A medium (Invitrogen) two times, to acquire a single cell suspension. Then, the cells were centrifuged for 5 min at 300g and resuspended in neurobasal A medium supplemented with 2 mM L-glutamine, 1% N-2 supplement (100x) (Invitrogen), 20 ng/ml epidermal growth factor (EGF) (ImmunoTools, Friesoyhte, Germany), 20 ng/ml basic fibroblast growth factor (bFGF) (ImmunoTools), 100 U/ml penicillin and 100 µg/ml streptomycin (referred to as standard NSC medium). The cell suspension was rinsed through a 70 µm cell strainer prior to seeding the cells in a T25 culture flask. The cells were cultured for about five days (37°C, 5% CO_2), allowing the NSCs to form floating spheres. Simultaneously, unwanted cell types expanded and adhered to the plastic surface of the culture flask. Both EGF and bFGF were added to the culture every other day. Subsequently, the medium containing the free floating NSC spheres was collected and centrifuged for 5 min at 200g. The pelleted spheres were incubated with accutase (Sigma) for 5 min (37°C) to obtain a single cell suspension. Then, NSCs were seeded at a density of 2 x 10^4 cells/cm^2 in T25 flasks coated with 3 µg/ml fibronectin (R&D systems) to allow adherence of NSCs and formation of colonies (37°C, 5% CO_2). The culture medium was changed every 3 to 4 days and cells were sub-cultured when about 80% confluence was reached. To passage the cells, NSCs were harvested by incubation with accutase for 5 minutes (37°C) and centrifuged for 5 min at 300g. Subsequently, cells were resuspended in standard NSC culture medium and seeded at a density of 2 x 10^4 cells/cm^2 in fibronectin coated culture flasks. Mouse NSCs were stored at -80°C in standard NSC medium supplemented with 10% DMSO. Temperature was gradually reduced at a rate of 1°C per min, using a CoolCell container. For immunocytochemical analysis, the NSCs were seeded at 2 x 10^4 cells/cm^2.

2.6 Culture of human embryonic stem cells

Human H9 embryonic stem cells were obtained from the stem cell institute of KU Leuven (SCIL) and cultured using the standard feeder-dependent method. Prior to seeding the cells, 6-well plates were coated with 0.1% gelatine and plated with Mitomycin-C treated CF-1 mouse embryonic fibroblasts (MEFs) (AMS biotechnology, Abingdon, United Kingdom) at a density of 2,5 x 10^4 cells/cm^2 in DMEM high glucose medium (Invitrogen) supplemented with 15% FBS, 4 mM L-glutamine, 10 U/ml penicillin, 10 µg/ml streptomycin, 2% Non-Essential Amino Acids (NEAA) (Invitrogen) and 100 µM β-mercaptoethanol (Gibco). The MEFs were incubated overnight to allow attachment of the cells to the surface of the culture plate (37°C, 5% CO_2). Consequently, H9 ESCs were cultured in MEF-seeded 6-well plates in DMEM/F12 medium (Invitrogen) supplemented with 20% knock-out serum replacement (Gibco), 1 mM L-glutamine, 10 U/ml penicillin, 10 µg/ml streptomycin, 100 µM NEAA, 0.1 mM β-mercaptoethanol (Sigma) and 4 ng/ml bFGF (referred to as standard hESC medium) (37°C, 5% CO_2). Purity of the cell culture was maintained by daily medium change and removal of aberrant colonies, using a VACUBOY aspiration system (Integra Biosciences, Hudson, United States of America). Sub-culture of H9 ESCs was performed when optimal colony density and size was reached. Hereby, the cells were washed with PBS and incubated with 1 mg/ml collagenase IV (Invitrogen) in DMEM/F12 for 5 min (37°C, 5% CO_2). Thereafter, the collagenase IV solution was removed and cells were washed with standard hESC culture medium. After scraping, the cells were collected in a falcon tube and gently resuspended using a Pasteur pipet. Consequently, the cells were centrifuged at 200g for 5 min and gently resuspended in the appropriate volume of standard hESC medium. Cells were seeded on the coated 6-well plates with a splitting ratio varying between 1:1 and 1:4. Human H9 ESCs were stored at -80°C in standard hESC medium supplemented with 60% FCS and 20% DMSO. Temperature was gradually reduced at a rate of 1°C per min, using a CoolCell.

2.7 Immunocytochemistry

Immunocytochemical staining was performed on paraformaldehyde (PFA) fixed cells, using the diaminobenzidine (DAB) detection method or the fluorescence detection method. Cells were seeded at glass coverslips and fixed for 20 min with 4% PFA. Fixed cells were washed three times with PBS (0.01M, pH 7.2) and depending on the cellular location of the antigen, permeabilized with 0.05% triton (Boehringer, Mannheim, Germany) for 30 min at 4°C. Thereafter, cells were washed three times in PBS and blocking was performed for 20 min at room temperature to reduce non-specific binding of secondary antibodies. Depending on the secondary antibody, either 10% normal goat serum (Millipore) or 10% normal donkey serum (Millipore) was used. After blocking, the cells were washed three times with PBS and incubated with the primary antibody *(table 1)* for 1h at room temperature or overnight at 4°C. Prior to incubation with the secondary antibody, cells were washed four times with PBS.

2.7.1 Diaminobenzidine detection method

Using the DAB detection method, cells were incubated with horse radish peroxidase (HRP) labelled secondary antibodies *(table 1)* of the DAB EnVision kit (Dakocytomation, Glostrup, Denmark) for 30 min at room temperature. Subsequently, cells were washed four times with PBS and incubated with

DAB substrate and chromogen solution of the DAB EnVision kit for 1-10 min at room temperature. After nuclear counterstaining with hematoxylin/eosin solution, the coverslips were mounted on glass slides (Thermo-Scientific, Menzel-Gläser, Braunschweig, Germany) with Aquatex mounting medium (Merck, Darmstadt, Germany). Analysis was carried out using a Nikon eclipse 80i microscope (Tokyo, Japan) with compatible LENet software or a Mirax Desk digital slide scanner (Zeiss, Oberkochen, Germany) with Mirax scan software.

2.7.2 Fluorescence detection method

Using the fluorescence detection method, cells were incubated with fluorophore labelled secondary antibodies *(table 1)* for 30 min at room temperature. After washing with PBS four times, nuclei were stained with 4',6-diamidino-2-phenylindole (DAPI) for 10 min at room temperature. Thereafter, cells were washed 3 times with PBS and coverslips were mounted on glass slides with anti-fade mounting medium (Dakocytomation). Analysis was performed using a Nikon eclipse 80i microscope and NIS Elements BR 3.10 software.

Table 1: antibodies used for immunostainings

Target	Host	Conjugate	Dilution	Clone	Supplier	Ref nr
Primary antibodies						
Nanog	Rabbit	-	1/250	EPR2027	Abcam	Ab109250
Sox2	Rabbit	-	1/1000	Polyclonal	Abcam	Ab97959
Sox2	Rabbit	-	1/1000	Polyclonal	Millipore	AB5603
Oct-4	Rabbit	-	1/1000	Polyclonal	Abcam	Ab19857
Tra-1-60	Mouse	-	1/1000	Tra-1-60	Millipore	MAB4360
Tra-1-81	Mouse	-	1/1000	Tra-1-81	Millipore	MAB4381
CXCR4	Mouse	-	1/25	12G5	BioLegend	306502
CXCR4	Rat	-	1/50	247506	R&D systems	21651-100
SDF-1	Mouse	-	1/500	K15C	Millipore	MABC184
BLBP	Rabbit	-	1/250	Polyclonal	Millipore	ABN14
PDGF-Rα	Rat	-	1/100	APA5	Novus Bio	NBP1-43350
Tuj1	Rabbit	-	1/50	Polyclonal	Abcam	Ab18207
NeuN	Mouse	-	1/100	A60	Millipore	MAB377
Secondary antibodies						
Mouse IgG	Goat	HRP	RTU	Polyclonal	Dako	K4007
Rabbit IgG	Goat	HRP	RTU	Polyclonal	Dako	K4011
Rat IgG	Donkey	AF488	1/500	Polyclonal	Jackson	712-545-150
Rabbit IgG	Donkey	AF488	1/500	Polyclonal	Life tech	A21206
Mouse IgG	Donkey	AF555	1/500	Polyclonal	Life tech	A31570

HRP = horse radish peroxidase, RTU = ready to use, AF = alexa fluor

2.8 Immunohistochemistry

Immunohistochemical staining of post-stroke brain tissue was performed on PFA fixed, paraffin embedded sections. Eight week old mice (C57Bl/6) were subjected to transient middle cerebral artery occlusion (tMCAO) for 30 min. to induce a stroke lesion as approved by the ethical committee (protocol number 201428). One week post-tMCAO, the mice were sacrificed and the brain was fixed

by means of transcardial perfusion with 4% PFA, isolated and exposed to 4% PFA for 24h. Fixed brains were embedded in paraffin after they were dehydrated by exposure to increasing concentrations of ethanol solutions and xylene. Sections of 7 µm were cut with a microtome. Prior to staining, paraffin embedded sections were exposed to xylene and decreasing concentrations of ethanol and washed in PBS. Heat-induced antigen retrieval was performed by heating the sections in citrate buffer (Dako) for 10 min, using a microwave oven (480W). To reduce non-specific staining by endogenous peroxidase, sections were incubated with peroxidase block solution (Dako) for 30 min. at room temperature. Thereafter, blocking for non-specific binding was performed by incubating the sections with 10% normal goat serum (Millipore) for 20 min. Consequently, the cells were washed three times with PBS and incubated with the primary antibody *(table 1)* for 1h at room temperature or overnight at 4°C. Prior to incubation with the HRP-labeled secondary antibodies *(table 1)* for 30 min, cells were washed three times with PBS. After incubation with secondary antibodies, sections were washed three times with PBS and exposed to DAB/chromogen solution of the DAB EnVision kit for 1-6 min. at room temperature. Sections were counterstained with hematoxylin for 3 min. Finally, sections were dehydrated and coverslips were mounted using DPX medium. Analysis was carried out using a Mirax Desk digital slide scanner with Mirax scan software.

2.9 Flow cytometry

Flowcytometric analysis was performed on NSCs. Therefore, NSCs were dissociated with accutase and washed in FACS-buffer. After washing, the cells were incubated at room temperature for 30 min to allow epitope recovery. Consequently, the primary antibodies were incubated for 45 min. at room temperature *(table 2)*. If unlabelled primary antibodies were used, the cells were also incubated with a secondary antibody conjugated with a fluorescent label for 30 min. after the cells were washed three times with FACS buffer. Finally, the cells were washed two times in FACS buffer and analysed with the BD FACSCalibur System, using BD CellQuest Pro Software.

Table 2: antibodies and isotypes used for flow cytometric analysis

Target	Host	Conjugate	Dilution	Clone	Supplier	Ref nr
Primary antibodies						
CD45	Rat	PE	1/100	30F-11	BD bioscience	553081
Sca-1	Rat	PE	1/200	D7	eBioscience	12-5981
A2B5	Mouse	-	1/100	A2B5-105	Millipore	MAB312
NCAM	Rabbit	-	1/100	Polyclonal	Millipore	Ab5032
Secondary antibodies						
Rabbit IgG	Goat	AF488	1/200	Polyclonal	Life tech	A11008
Mouse IgG_1	Goat	AF488	1/200	Polyclonal	Life tech	A21121
Isotypes						
	Rat $IgG_{2\beta\kappa}$	PE	1/100	10H5	eBioscience	12-4031
	Mouse IgM	FITC	1/100	11E10	eBioscience	9011-4752

PE = Phycoerythrin, AF = Alexa fluor, FITC = Fluorescein isothiocyanate.

2.10 Transmission electron microscopy

Transmission electron microscopy was used for the ultrastructural analysis of cells. Therefore, cells were seeded on Thermanox coverslips and fixed with 2% glutaraldehyde in 0,05 M sodium cacodylate buffer (Aurion, Wageningen,The Netherlands) at 4°C. The cells were washed with 0.05 M sodium cacodylate buffer and 0.15 M sacharose prior to post-fixation with 2% osmiumtetroxide (Aurion) in 0.05 M sodium cacodylate buffer for 1h at 4°C. Consequently, dehydration was achieved by exposure to ascending concentrations of acetone and cells were impregnated overnight with 50% araldite epoxyresin (Aurion) in acetone at room temperature. Thereafter, cells were embedded in araldite epoxy resin by means of the pop-off method (60°C). Using a Leica EM UC6 microtome, slices (40-60 nm) were cut from the embedded sample and transferred to 0.7% formvar-coated copper grids (Aurion). The cells were contrasted with 0.5% uranyl acetate and lead citrate solution. Ultrastructural analysis was performed with a Phillips EM208 S transmission electron microscope (80 kV), equipped with a Morada Soft Imaging System camera. Digital processing of the obtained images was performed with iTEM-FEI software (Olympus SIS, Münster, Germany).

2.11 Statistical analysis

Statistical analysis was performed with Graphpad Prism 5 software. Significant differences in the neurite analysis experiment were tested by means of the Kruskal-Wallis test and Dunn's multiple comparison test. Data represent mean values ± standard deviation (SD).

3 Results

In the following sections the results of this study are provided. These include the establishment and characterization of a NSC culture as well as a pCN culture and morphological analysis of hDPSCs. Furthermore, the identification of the CXCR4 migratory pathway in hDPSCs and optimization of an OGD survival assay is discussed. Additionally, a H9 hESC culture is morphologically analysed.

3.1 Morphology of human dental pulp stem cells

The hDPSCs used in this study are obtained by means of an explant culture *(fig. 1A)*. The dental pulp tissue adheres to the surface of the culture plate and hDPSCs proliferate and grow out of the explant, resulting in an adherent culture of hDPSCs *(fig. 1B).* A standard hDPSC culture is a morphologically heterogeneous population of cells comprising cells that can range from spindle-like shaped to polygonal shaped with variable extensions. Ultrastructural analysis of hDPSCs shows cells with large nuclei containing prominent nucleoli. The perinuclear region is an organelle-rich zone with various mitochondria, rough endoplasmic reticulum and Golgi complexes *(fig. 1C and 1D).* The peripheral zone of the cytosol is electron-lucent due to the absence of organelles.

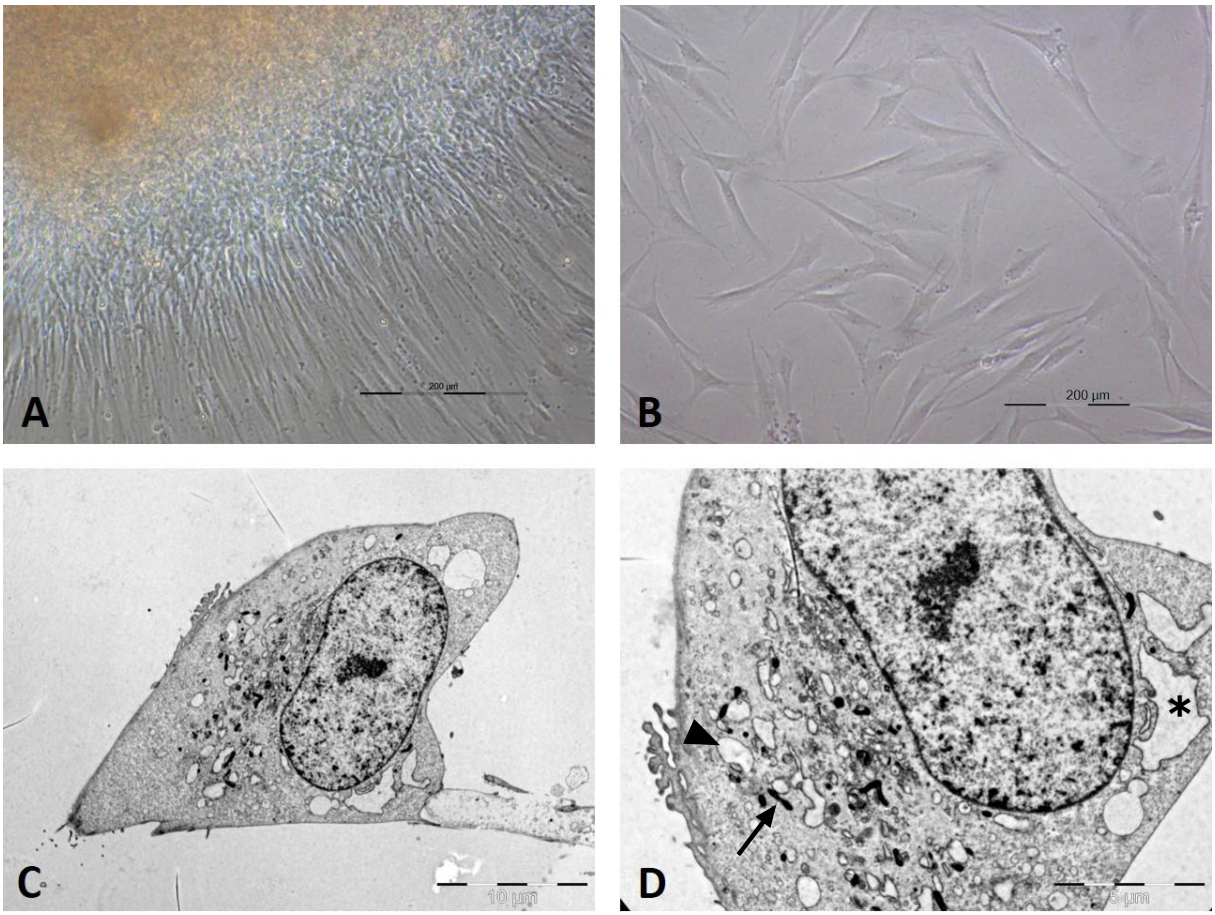

Figure 1: Morphological analysis of hDPSCs.
(A) hDPSCs proliferate and migrate out of the explant. **(B)** Morphological heterogeneity is observed in the hDPSC culture. Cell morphology ranges from spindle-like shaped to polygonal shaped with variable extensions. **(C)** Ultrastructural image of a hDPSC. The perinuclear zone is defined as an organelle-rich region, while the peripheral zone is electron-lucent. **(D)** At higher magnification, a large euchromatic nucleus with prominent nucleoli and a perinuclear region with mitochondria (arrow), rough endoplasmic reticulum (triangle) and Golgi complex (*****) is observed (scale bar A,B = 200 µm, C = 10 µm and D = 5 µm).

3.2 Isolation, culture and characterization of mouse neural stem cells

In order to investigate the potential neuroregenerative effects of hDPSCs *in vitro*, mouse NSCs are used since they are essential in the process of neuroregeneration. Therefore, an NSC culture needed to be established and characterized. Mouse NSCs were isolated from the brains of mouse foetuses and initially cultured as neurospheres *(fig. 2A).* While the NSCs form neurospheres, other unwanted cell types (e.g. fibroblasts, glial cells, endothelial cells etc.) adhere to the surface, remain latent in culture or are negatively selected because of a lack of the appropriate supporting factors. Consequently, neurospheres were dissociated and the obtained single cells were cultured in fibronectin-coated flasks to allow adherent cell culture *(fig. 2B-D).* Occasionally, persisted unwanted cell types were observed as shown by a fibroblast-like morphology. However, their presence decreased with rising passage numbers. The NSCs typically acquired a bipolar or multipolar morphology with extensions that appeared to seek contact with the surrounding cells. NSCs derived from 11 different foetuses were cultured separately and are considered as distinct cell-lines.

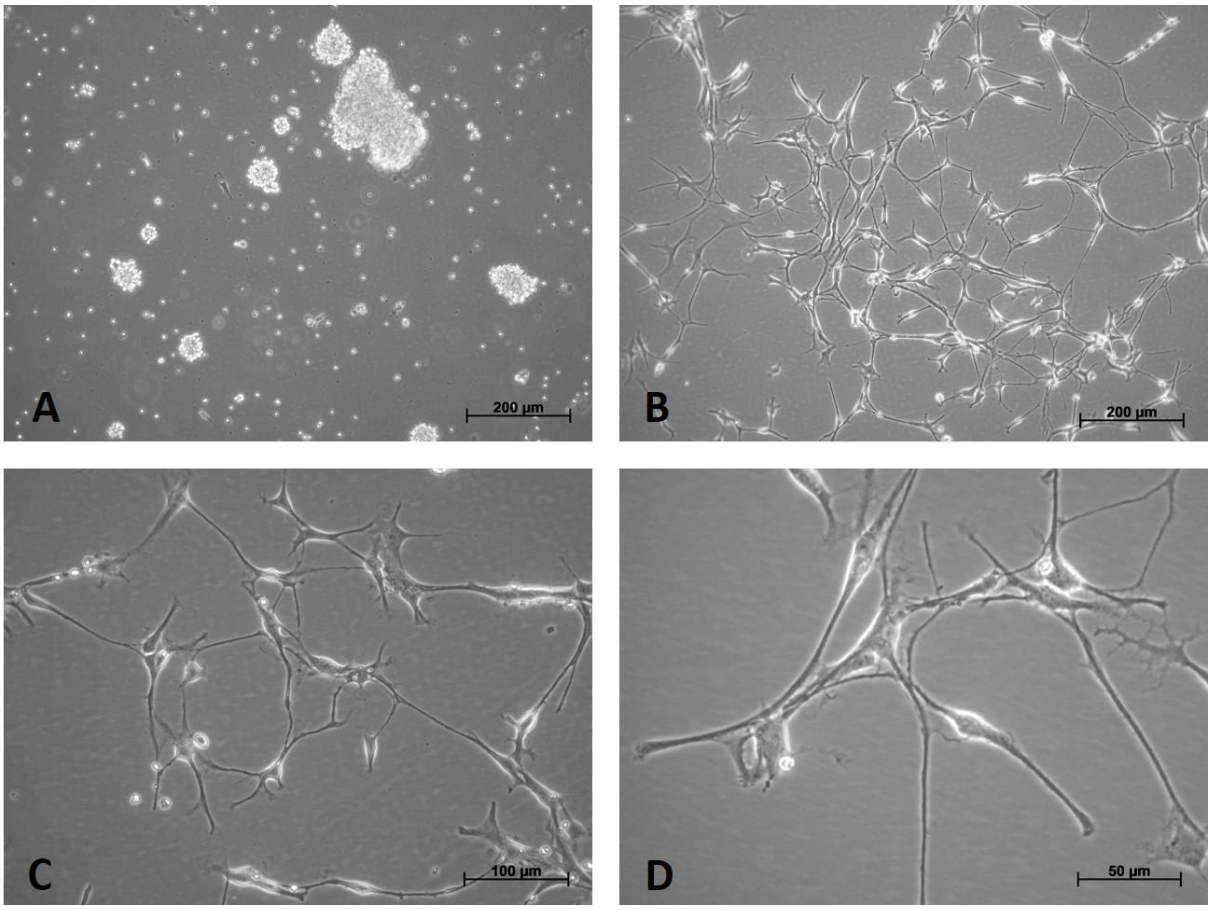

Figure 2: Phase-contrast images of mouse NSC culture.
(A) Following isolation, NSCs were cultured in uncoated culture flasks resulting in neurospheres formation (scale bar = 200 µm). **(B-D)** From passage 1, single cells were seeded in fibronectin-coated flasks to allow adherent culture. NSCs had a bipolar or multipolar morphology with extensions that seemed to seek contact with surrounding cells (scale bar B = 200 µm, C = 100 µm, D = 50 µm).

3.2.1 Phenotypic characterization of mouse neural stem cells

The NSCs were phenotypically characterized by means of immunocytochemical analysis *(fig. 3).* The isolated NSCs show homogeneous expression of brain lipid-binding protein (BLBP) in the cytoplasm. Staining for Sox2 resulted in reactivity in the nucleus and in the perinuclear region, but not in the cellular extensions. Furthermore, the NSCs showed low expression of the platelet-derived growth factor receptor alpha (PDGF-Rα) on the cell membrane. No expression of β3-tubulin (Tuj1) and NeuN was observed. All stainings were performed on three NSC lines.

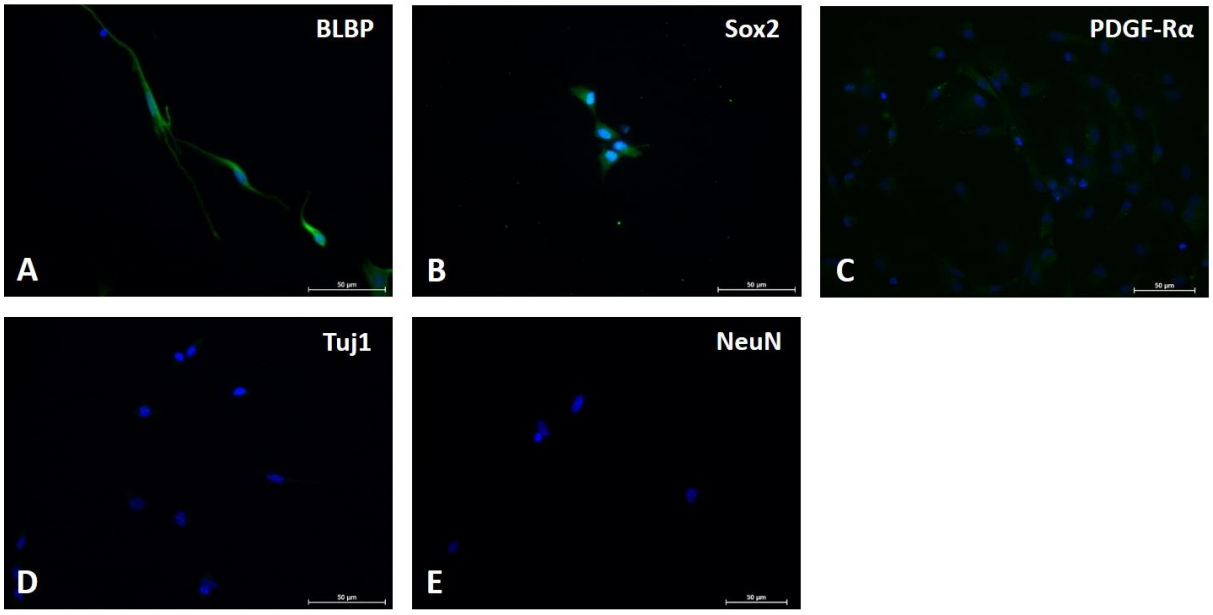

Figure 3: Immunocytochemical analysis of stem cell markers in NSCs.
(A and **B)** Immunofluorescence stainings showed that NSCs expressed BLBP and Sox2. Presence of Sox2 was observed in the nucleus and the perinuclear region, but not in the extensions. **(C)** Only weak reactivity could be observed for the PDGF-Rα. **(D** and **E)** NSCs were negative for Tuj1 and NeuN. Stainings were performed on three NSC lines (scale bar = 50 µm).

Additionally, a flow cytometric analysis was performed to evaluate the expression of CD45, stem cell antigen 1 (Sca-1), neural cell adhesion molecule (NCAM) and A2B5. NSCs showed that no expression of CD45 and Sca-1 and only 7.57% (SD = 3.70%) and 11.45% (SD = 3.9%) were positive for A2B5 and NCAM respectively *(data not shown)*. Three NSC lines were used for analysis.

3.3 Identification of the CXCR4/SDF-1 migratory pathway in hDPSCs

To investigate the migratory potential of hDPSCs in the context of stroke, the presence of the chemokine receptor CXCR4 in hDPSCs was investigated. Immunocytochemical analysis revealed that hDPSCs expressed the CXCR4 receptor *(fig. 4).* Furthermore, a polarity in the distribution of CXCR4 on the cell surface was observed. Analysis of hDPSCs of 6 different donors showed that 96.51% (SD = 4.58%) of the hDPSCs displayed immune-reactivity for CXCR4.

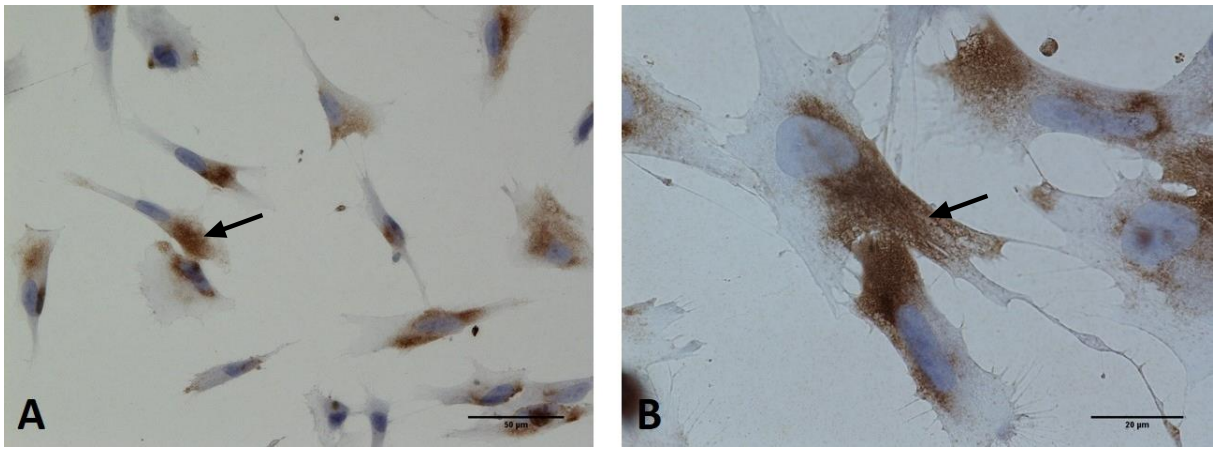

Figure 4: hDPSCs express the CXCR4 receptor.
(A) Immunocytochemical analysis revealed that hDPSCs expressed CXCR4 (scale bar = 50 µm). **(B)** Furthermore, a polarity in the distribution of CXCR4 on the cell surface was observed (arrow) (scale bar = 20 µm).

Since NSCs play a crucial role in the process of neuroregeneration, the presence of the CXCR4 receptor in NSCs was investigated. Immunocytochemical analysis showed the presence of CXCR4 on the cell surface of NSCs *(fig. 5A).* Furthermore, no expression of SDF-1 by hDPSCs could be observed *(fig. 5C).* Staining for CXCR4 in hDPSCs was also performed using the fluorescence detection method. As demonstrated with the DAB staining, the hDPSCs showed immune-reactivity for CXCR4 *(fig. 5B).*

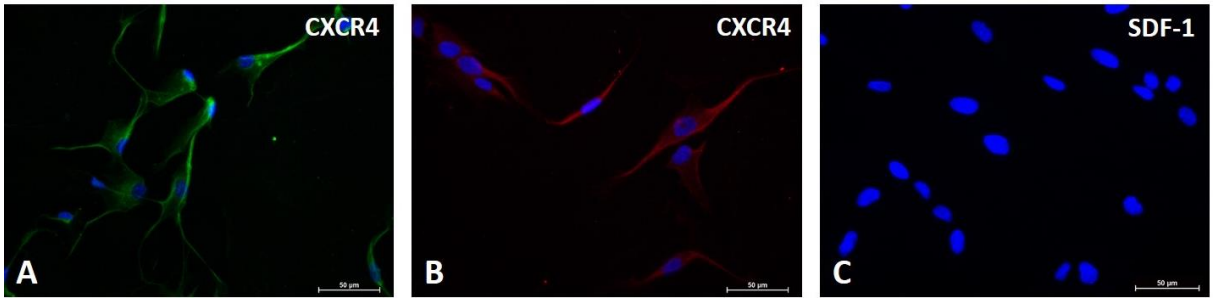

Figure 5: NSCs and hDPSCs express the CXCR4 receptor.
(A) Immunofluorescent staining of NSCs showed that they express the CXCR4 receptor. **(B)** Staining for CXCR4 in hDPSCs was also performed using the fluorescence detection method and the hDPSCs were found to be positive for CXCR4. **(C)** Furthermore, an SDF-1 staining in hDPSCs showed that they did not express SDF-1 (scale bar A, B and C = 50 µm).

3.4 Isolation and culture of mouse cortical neurons

To investigate potential neuroprotective effects of hDPSCs *in vitro,* mouse pCNs are used since cortical neurons are the main cells that are affected in stroke. Therefore, a pCN culture had to be optimized. The pCNs were isolated from cortices of foetal mice and cultured in poly-d-lysine coated culture plates. In order to obtain the optimal cell density, pCNs were seeded at cell densities varying from 3 x 10^4 cells/cm^2 to 2.4 x 10^5 cells/cm^2. Consequently, the cell culture was allowed to maturate for 5 days prior to analysis *(fig. 6).* When the pCNs were seeded at 3 x 10^4 cells/cm^2, they stayed in culture as single cells and had a round-shaped or bipolar morphology with short extensions. At 6 x 10^4 cells/cm^2, the cells started to aggregate and form neurites that extended to the periphery of the aggregate. Seeding the cells at 1.2 x 10^5 cells/cm^2 resulted in a culture with the formation of strong connections between the aggregates, together with smaller neurites which probed the vicinity of the aggregates. At 2.4 x 10^5 cells/cm^2, similar results were obtained. However, the aggregates seemed to be larger. Occasionally, non-neuronal cell types could be observed in the culture. These cells often displayed a fibroblast-like morphology. Primary CNs could be kept in culture for 2 weeks without having a significant reduction in culture quality. Performing experimental procedures that required changing of the medium of the pCN culture showed that the cultures were sensitive to mechanical forces, since the pCNs partially detached after each medium change. Albeit, the cultures with higher densities (>1.2 x 10^5 cells/cm^2) seemed to be more resistant against the mechanical forces. Taken together, a stable pCN culture could be established. In this culture, the pCNs aggregate and form a strong neuronal network with the surrounding aggregates.

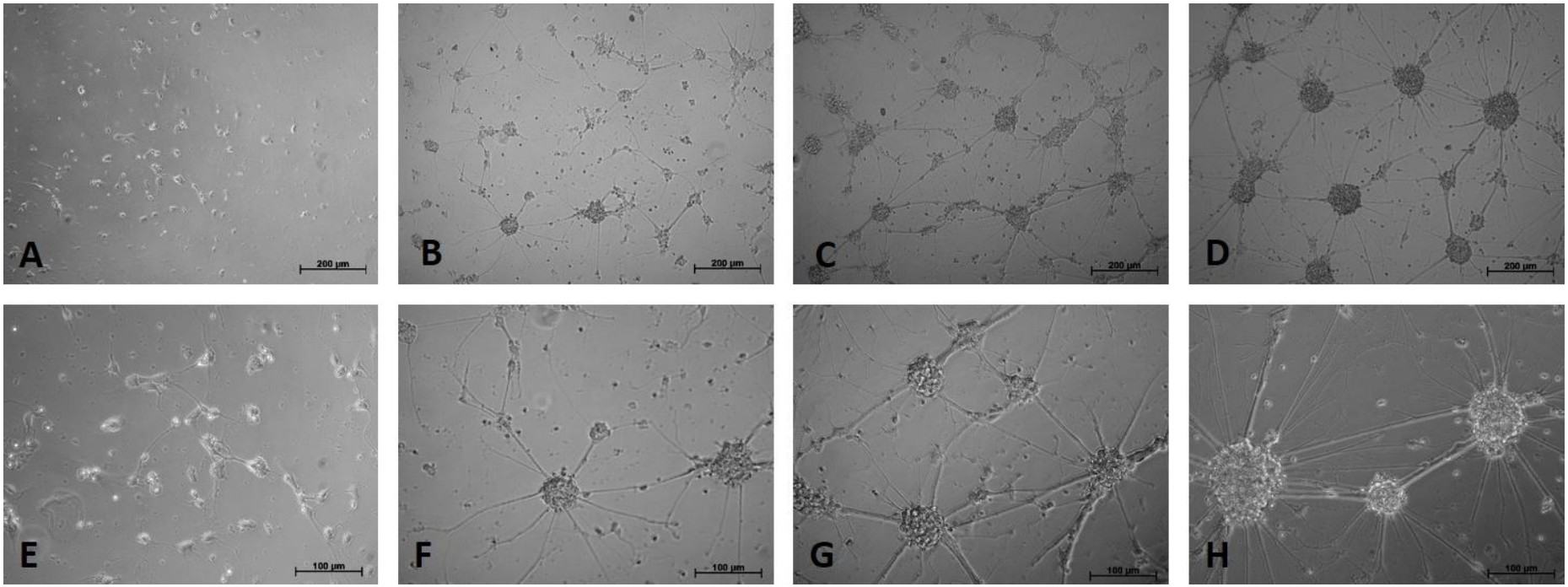

Figure 6: Phase-contrast images of pCNs in culture at varying cell densities.
Isolated pCNs were seeded at varying cell densities on poly-d-lysine coated culture plates and cultured for 5 days to allow maturation of the neuron culture. **(A** and **E)** When cells were seeded at 3 x 10^4 cells/cm^2 the cells showed a round-shaped or bipolar morphology with short extensions. **(B** and **F)** At 6 x 10^4 cells/cm^2 the cells started to aggregate and form neurites that extended to the periphery of the aggregate. **(C** and **G)** At 1.2 x 10^5 cells/cm^2 strong connections between the aggregates could be observed together with smaller neurites that were probing the vicinity of the aggregates. **(D** and **H)** At 2.4 x 10^5 cells/cm^2 similar results were obtained, however the aggregates seemed to be larger (scale bar A-D = 200 µm and E-H = 100 µm).

3.5 Optimization of an oxygen-glucose deprivation survival assay

In order to evaluate the capacity of hDPSCs to exert a neuroprotective effect an oxygen-glucose deprivation (OGD) survival assay is developed *(fig. 7).* This assay will allow the viability of pCNs that have been exposed to cell death-inducing stress followed by exposure to the CM of the hDPSCs to be measured. To ensure a reliable survival assay will be available, the AlamarBlue® viability assay was validated and the OGD exposure time was optimized.

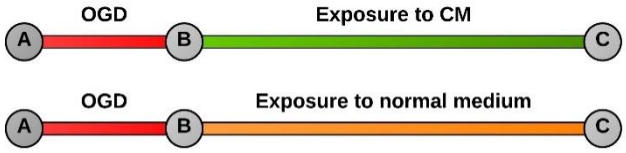

Figure 7: Experimental setup of the OGD survival assay.
The pCN culture is exposed to OGD for a determined time period (A to B). After OGD the pCNs are exposed to either the normal medium or the conditioned medium (CM) of hDPSCs. Cell viability is measured at the starting point (A), after OGD (B) and 24h after OGD (C).

3.5.1 Validation of the AlamarBlue® viability assay in mouse cortical neurons

Validation of the AlamarBlue® assay for measuring cell viability in pCNs was performed. The pCNs were seeded at 1.5 x 10^4 cells/cm^2, 3 x 10^4 cells/cm^2, 6 x 10^4 cells/cm^2, 1.2 x 10^5 cells/cm^2 and 2.4 x 10^5 cells/cm^2 and cultured in standard pCN medium for 5 days. The fluorescence intensity (FI) was measured after 2h, 3h, 4h and 6h of incubation with the AlamarBlue® dye *(fig. 8).* A linear correlation was observed between cell density and FI. With increasing cell density more of the AlamarBlue® dye was metabolized, resulting in a more intense fluorescence signal. Furthermore, with increasing incubation time the fluorescence signal was more intense for a given cell density. These findings imply that the AlamarBlue® assay is an accurate tool to measure the metabolic activity of pCNs in culture, which can be used as an indication for cell viability.

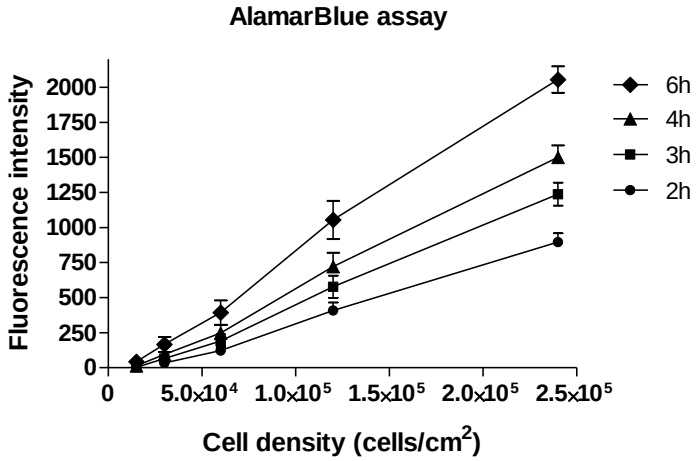

Figure 8: Optimization of the AlamarBlue® viability assay in pCNs.
The pCNs were seeded at cell densities varying from 1.5 x 10^4 cells/cm^2 to 2.4 x 10^5 cells/cm^2 and cultured in standard pCN medium for 5 days. After adding the AlamarBlue® dye, the FI was measured after 2h, 3h, 4h and 6h of incubation. FI was measured at 590 nm with excitation at 540 nm and corrected for the inherent fluorescence of the medium (n = 3).

3.5.2 Optimization of the oxygen-glucose deprivation exposure time

To acquire optimal results with the OGD survival assay, the OGD exposure time had to be optimized. The metabolic activity of the pCNs was measured after exposure to OGD for varying time periods in order to evaluate the cell viability. Following isolation, the pCNs were seeded at a density of 6 x 10^4 cells/cm^2 and cultured in standard pCN medium to allow maturation of the neuronal culture. OGD was induced by incubating the pCN culture in DMEM without glucose in a hypoxic environment (0% O_2, 5-10% CO_2). The pCNs were exposed to OGD for 1h, 3h and 24h and consequently incubated with either standard pCN medium or α-MEM supplemented with 0.1% FBS. The metabolic activity was evaluated immediately after OGD and 24h after OGD, with the AlamarBlue® viability assay. The experiment was performed in triplicate and correction for the inherent fluorescence of the medium was taken into account.

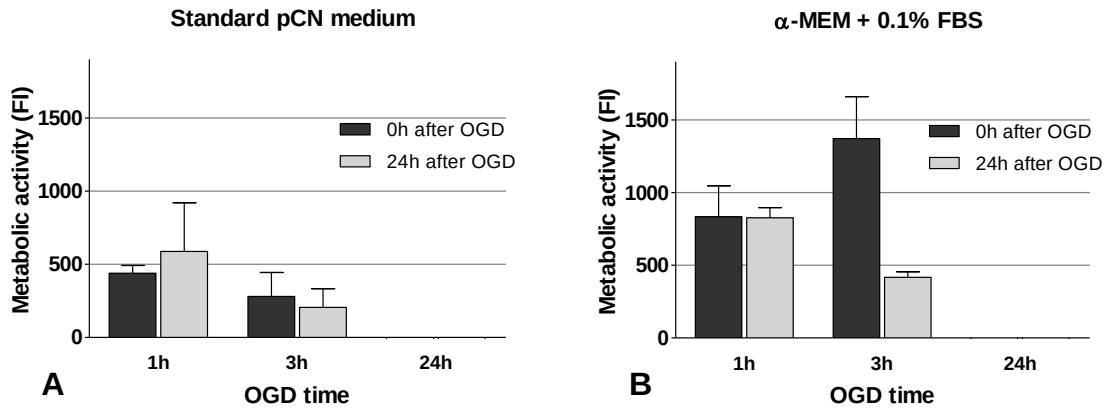

Figure 9: Optimization of the oxygen-glucose deprivation exposure time.
The pCNs were exposed to 1h, 3h and 24h of OGD and consequently incubated with either standard pCN medium or α-MEM supplemented with 0.1% FBS. The metabolic activity was measured immediately after OGD and 24h after OGD with the AlamarBlue® viability assay. **(A)** After 1h of OGD the FI is 438.7 (SD = 54.5) when measured immediately after OGD and 588.3 (SD = 331.5) when measured 24h later. After 3h of OGD the metabolic activity of the cells seemed to be reduced. 24h of OGD resulted in a complete abolishing of metabolic activity. **(B)** In the condition with α-MEM + 0.1% FBS, a higher metabolic activity was observed after 1h and 3h of OGD. The FI after 1h of OGD was 834.7 (SD = 212.9) and 24h later 826.7 (SD = 69.7). Remarkably, after 3h of OGD a higher metabolic activity (1373, SD = 287.9) was observed than after 1h OGD. However, 24h later the metabolic activity dropped drastically (417.7, SD = 37.8).

In the condition with standard pCN medium, a FI of 438.7 (SD = 54.5) was measured immediately after 1h of OGD. 24h later a FI of 588.3 (SD = 331.5) is observed *(fig. 9A).* After 3h of OGD the metabolic activity of the cells seemed to be reduced. A FI of 279 (SD = 165.4) and 206.7 (SD = 125.9) was measured, respectively after 3h OGD and 24h later. 24h of OGD resulted in a complete abolishing of metabolic activity, which suggests that all cells were dead. In the condition with α-MEM supplemented with 0.1% FBS, a higher metabolic activity was detected after 1h and 3h of OGD compared to the condition with pCN medium *(fig. 9B).* The FI after 1h of OGD was 834.7 (SD = 212.9) and 24h later 826.7 (SD = 69.7). Remarkably, after 3h of OGD a higher metabolic activity (1373, SD = 287.9) was observed than after 1h OGD. However, 24h later the metabolic activity dropped drastically (417.7, SD = 37.8). After 24h of OGD, the cells show no sign of metabolic activity.

Since the AlamarBlue® assay measures the metabolic activity, which is an indirect indication for cell viability, an annexin V/PI flowcytometric apoptosis assay was performed to investigate whether actual cell death was present in the pCN culture. Therefore, pCNs were subjected to 1h and 3h of OGD and immediately after OGD cell death was evaluated by means of the flowcytometric apoptosis assay *(fig. 10).* A low percentage of cell death was observed after 1h of OGD (3.21%) and 3h of OGD (6.51%). However similar amounts of dying cells were observed in the control condition (5.52%). These findings suggest that 1h and 3h of OGD does not induce significant cell death.

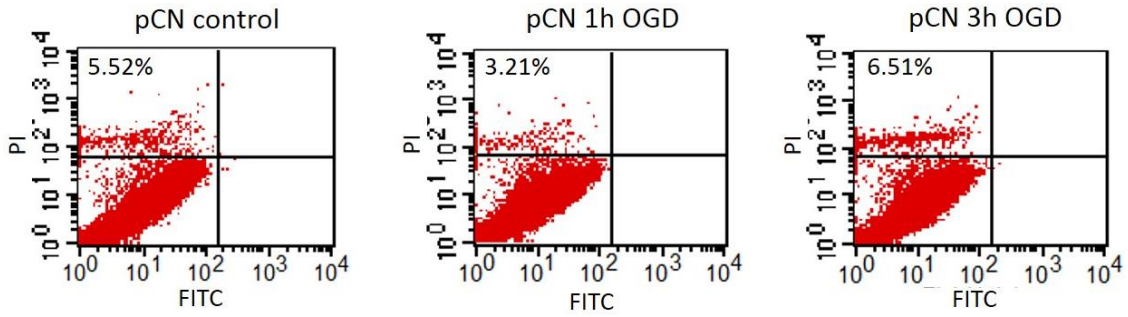

Figure 10: Flowcytometric analysis of cell death in pCNs after OGD.
The pCNs were subjected to 1h and 3h of OGD and immediately after OGD cell death was evaluated by means of the annexin V/PI flowcytometric apoptosis assay. Some cell death was observed after 1h of OGD (3.21%) and 3h of OGD (6.51%), however similar amounts of dying cells were observed in the control condition (5.52%).

In analogy with the OGD survival assay, the AlamarBlue® assay was carried out in a glutamate excitotoxicity model in which an extensive range of exposure times and glutamate concentrations were applied *(Supplemental information fig. S1)*. The results obtained in this experiment did not show a clear correlation between exposure time and glutamate concentration. Therefore, no supplementary annexin V/PI flowcytometric apoptosis assay was performed.

3.6 Effect of conditioned medium of hDPSCs on neurite outgrowth in pCNs

To investigate whether the secretome of hDPSCs has an effect on neurite outgrowth in pCNs, a neurite analysis was performed after exposure to the CM of hDPSCs. The pCNs were seeded on poly-d-lysine coated coverslips at 3 x 10^4 cell/cm^2. After 24h, the pCNs were exposed to the CM of hDPSCs of three different donors (P159, P160 and P162) for 96h. Consequently, the pCNs were fixed with 4% PFA and stained for Tuj1 to visualize the cytoskeleton of the neurons to allow analysis of the neurites. Standard pCN medium was used as a control. No significant difference in average neurite length could be observed between the pCNs exposed to the control medium and the CM of the hDPSCs *(fig. 11A).* The pCNs in the control condition had an average neurite length of 114.4 µm (SD = 15.5). The pCNs which were exposed to the CM of P159, P160 and P162 had an average neurite length of 113.5 µm (SD = 8.0), 117.4 µm (SD = 8.4) and 123.2 µm (SD = 9.9) respectively. Furthermore, the CM of the hDPSCs had no significant effect on the amount of neurites per cell *(fig. 11B).* The average amount of neurites per cell was 2.79 (SD = 0.01) in the control condition, while the average was 2.62 (SD = 0.05), 2.61 (SD = 0.07) and 2.60 (SD = 0.08) in the CM of hDPSCs of P159, P160 and P162 respectively. The experiment was performed on three different coverslips.

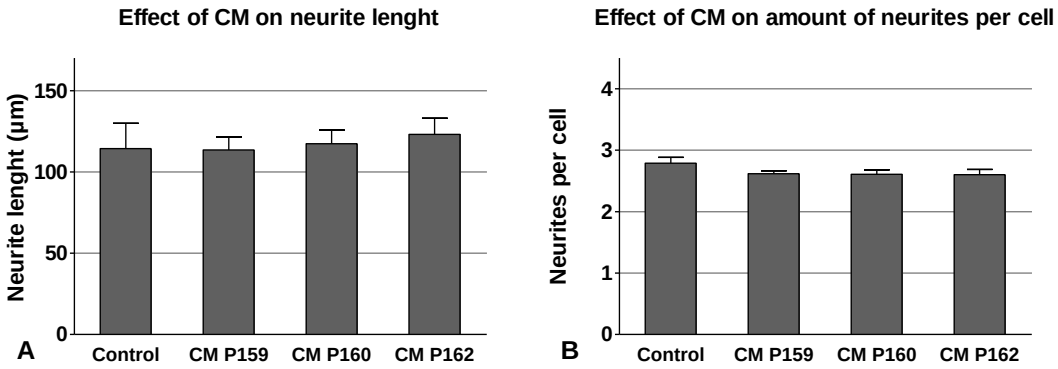

Figure 11: Effect of conditioned medium of hDPSCs on neurite outgrowth in pCNs.
(A) Exposure to the CM of hDPSCs had no effect on the neurite length of the pCNs. **(B)** Furthermore, no significant difference in amount of neurites per cell could be observed between the control and the CM of hDPSCs. Significance was tested with the Kruskal-Wallis test followed by the Dunn's multiple comparison test (n = 3).

3.7 Characterization of H9 human embryonic stem cells

The therapeutic potential of iPSCs in stroke is also of great interest. Prior to introducing an iPSC culture in the lab, we commence with establishing an H9 hESC culture to gain experience in culturing pluripotent stem cells and to be able to compare the iPSC culture with an already established culture of pluripotent stem cells. Therefore, as a first step the H9 hESCs were morphologically and phenotypically characterized.

3.7.1 Expression of pluripotency markers in H9 human embryonic stem cells

A H9 hESCs culture was established and analysed for the expression of five hallmark pluripotency markers. Immunocytochemical analysis showed expression of the transcription factors Nanog, Oct-4 and Sox2 in the nucleus and the presence of the glycoproteins Tra-1-60 and Tra-1-81 on the surface of H9 hESCs *(fig. 12).* The stainings showed that the vast majority of the cells in the colony expressed these essential pluripotency markers, indicating an undifferentiated H9 hESC culture.

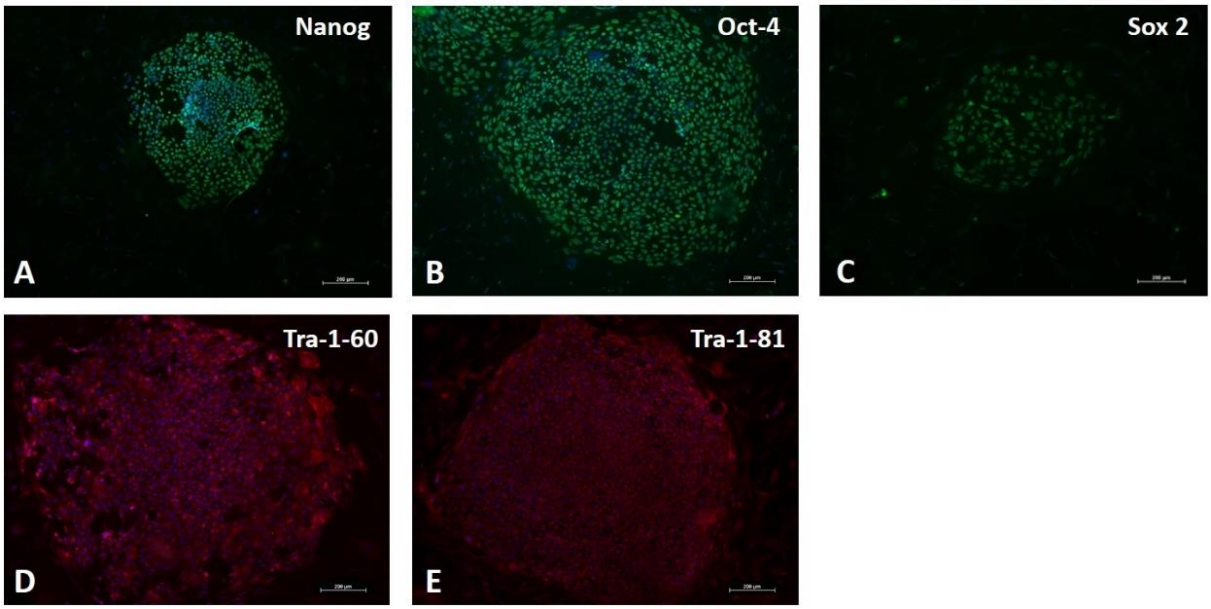

Figure 12: Immunocytochemical analysis of the expression of pluripotency markers in H9 hESCs.
(A-E) Immunofluorescence staining for Nanog, Oct-4, Sox-2, Tra-1-60 and Tra-1-81 shows that H9 hESCs were positive for all these pluripotency markers. Nuclear staining was performed with DAPI (blue) (scale bar=200 µm).

3.7.2 Morphology of H9 human embryonic stem cells

The H9 hESC culture was morphologically analysed. The pluripotent stem cells were cultured on mitotically inactivated feeder cells to maintain an undifferentiated pluripotent stem cell culture. They expanded in compact colonies which were demarcated by a defined border *(fig. 13A).* Ultrastructural analysis of the H9 hESC colonies showed that the cells were tightly packed and often made cell-cell contact. The cells typically had a high nucleus-to-cytoplasm ratio and a nucleus with prominent nucleoli. Only low amounts of cell organelles were detected in the cytoplasm. Mitochondria and endoplasmic reticulum were present in low numbers as well as some small vesicles. Golgi complexes were not observed *(fig. 13B-D).*

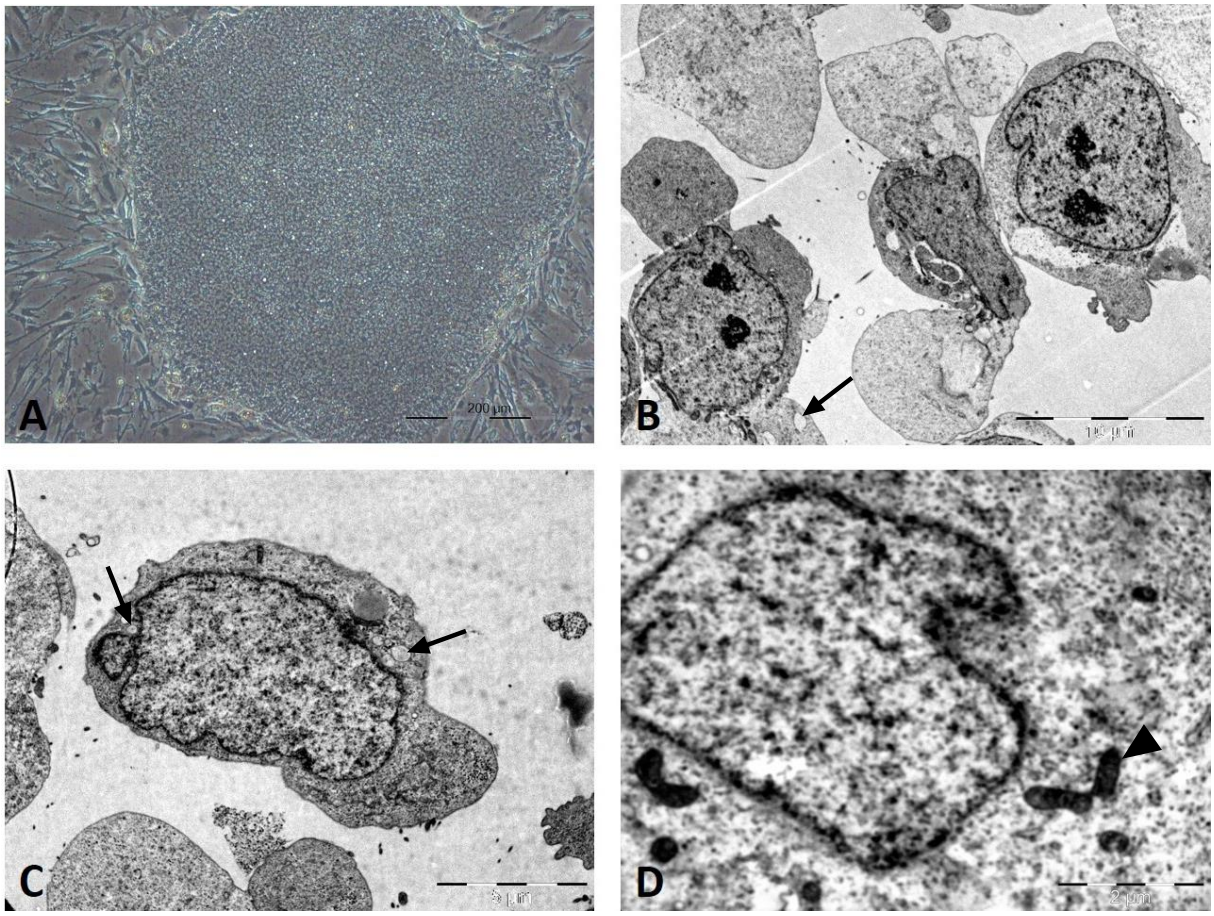

Figure 13: Morphological analysis of H9 hESCs.
(A) H9 hESCs grew in compact colonies on the feeder cell layer. The colonies had a defined border (scale bar = 200 µm). **(B)** Ultrastructural analysis of a H9 hESCs colony showed that the cells were tightly packed and often made cell-cell contact. The cells had a high nucleus-to-cytoplasm ratio and prominent nucleoli were observed (scale bar = 10 µm). **(C** and **D)** At higher magnifications, low numbers of cell organelles were detected. Certain mitochondria (triangle) are present and occasionally endoplasmic reticulum (arrow) and small vesicles were observed. Golgi complexes could not be detected (scale bar C = 5 µm and D= 2 µm).

4 Discussion

In order to develop an effective cell-based therapy for stroke, it is essential to have a profound understanding of the potential beneficial effects and underlying mechanisms of hDPSCs in stroke pathology. In this study, the goal is to identify neuroprotective and neuroregenerative effects of hDPSCs *in vitro* and their potential underlying mechanisms. To investigate the therapeutic potential of hDPSCs in the context of stroke in an *in vitro* setting, mouse pCNs and NSCs were isolated and culture conditions were optimized. Furthermore, the CXCR4/SDF-1 migratory axis is studied in hDPSCs and NSCs and the effects of the conditioned medium of hDPSCs on neurite outgrowth in pCNs is examined. Additionally, a H9 hESC culture is introduced in the lab to gain experience with a pluripotent stem cell culture for future experiments.

Due to previous research regarding hDPSCs that has been performed in our lab, a well-established hDPSCs culture is available. The culture conditions of the hDPSCs have been optimized and extensive characterization concerning morphology, ultrastructure, marker expression and differentiation potential of the hDPSCs has been performed [32, 58, 68]. For this study, hDPSCs were isolated from 7 different donors and all cultures displayed normal morphological properties.

Endogenous repair mechanisms including neurogenesis, neurite outgrowth and synaptogenesis are activated after stroke injury [17, 18]. However, these endogenous mechanisms are not potent enough to acquire adequate functional recovery in stroke patients. Stimulation of endogenous repair mechanisms in stroke patients could allow the brain to compensate the neuronal damage and restore the neurological function. Transplantation of rhesus monkey-derived DPSCs into healthy mouse brain showed to promote proliferation and differentiation of endogenous neural cells [67]. Additionally, a pilot study performed in our lab revealed that the CM of hDPSCs enhances neurite outgrowth in neuroblastoma cells (unpublished data). These findings indicate the potential of hDPSCs to have a neuroregenerative effect. To evaluate the capacity of hDPSCs to promote neurogenesis *in vitro*, NSCs will be used since they give rise to the neuronal cells in the brain. Therefore, a stable NSC culture needed to be established. The isolated NSCs were morphologically and phenotypically characterized to ensure a true NSC population was acquired. A NSC culture with typical morphological characteristics was observed and immunocytochemical analysis demonstrated that the isolated NSCs expressed BLBP, Sox2 and PDGF-Rα, but lacked the presence of Tuj1 and NeuN. In addition, a flow cytometric analysis (data not shown) showed no expression of CD45 and Sca-1 and only a small percentage of A2B5- and NCAM-positive NSC were observed. These observations are in line with previous reports of NSC cultures, with exception of the low expression of A2B5 and NCAM and the presence of the transcription factor Sox2 in the perinuclear region [69-71]. However, these irregularities are likely to be due to experimental error, since the complementary findings suggest the identity of a NSC culture. Nonetheless, it is recommended to repeat the phenotypical analysis for confirmation. Additionally, the differentiation capacity towards neurons, astrocytes and oligodendrocytes could be investigated to validate the NSC culture.

Regarding the evaluation of the potential of hDPSCs to exert neuroregenerative effects *in vitro*, the NSCs can be used to investigate the capacity of the secretome of hDPSCs to stimulate directed migration of NSCs and to induce differentiation of NSCs towards neuronal cell lineages.

Following transplantation, hDPSCs have to be able to migrate towards the site of injury to mediate their paracrine effects. Since it has been described that the CXCR4/SDF-1 pathway is important in the migration of NSCs towards the ischaemic lesion and the migration of BM-MSCs towards the stroke lesion, it is interesting to assess the role of this pathway in the migration of NSCs towards hDPSCs and of hDPSCs towards the ischaemic lesion [72, 73]. Immunocytochemical analysis in hDPSCs of 6 different donors revealed that the vast majority (97%) of the hDPSCs expressed the CXCR4 receptor. Moreover, a polarity in the distribution of the CXCR4 receptor on the cell surface was observed. A previous study already showed the presence of CXCR4 in a subpopulation of porcine-derived DPSCs [74]. The polarity may be explained by the secretion of certain factors by the surrounding cells. It has been described that various factors have an influence on the internalisation and externalisation of the CXCR4 receptor [75]. It can be speculated that the presence of the CXCR4 receptor is of great importance for the homing of the hDPSCs to the stroke lesion, since the CXCR4/SDF-1 axis regulates crucial steps in the transmigration of stem cells over the vessel wall and degradation of the basal membrane by controlling the secretion of MMPs [75, 76]. Furthermore, high SDF-1 production is observed in the stroke lesion, providing a signal for migration of hDPSCs towards the ischaemic lesion [72, 77]. To investigate the migration potential of hDPSCs towards SDF-1, a transwell migration assay is currently being optimized in our lab.

Moreover, attraction of NSCs towards hDPSCs could enhance endogenous neurogenesis. Immunocytochemical analysis showed strong expression of CXCR4 on the surface of the isolated NSCs. To be able to exert a chemoattractive effect via the CXCR4/SDF-1 axis, the hDPSCs should secrete SDF-1. Immunostaining in hDPSCs demonstrated that SDF-1 was not produced by these cells. This finding is in conflict with a previous study of Arthur *et al,* wherein was demonstrated that hDPSCs express SDF-1 on a transcriptional level and even secrete SDF-1 at a concentration of about 0.015 pg/cell [40]. Furthermore, induced secretion of SDF-1 in MSCs has already been described, using transfection methods. These SDF-1 enhanced MSCs did not display down regulation of their CXCR4 receptor and even showed increased survival compared to normal MSCs when exposed to hypoxia [78]. Moreover, these enhanced stem cells were still able to migrate towards the ischaemic lesion after transplantation in a rat model for myocardial infarction. The observation of increased survival of SDF-1 enhanced MSCs in hypoxic conditions is in line with a previous study that stated that SDF-1 stimulates proliferation and survival of MSCs [79]. Applying this method in hDPSCs would result in the generation of SDF-1 enhanced hDPSCs that display hypoxia-resistant properties and that could be able to stimulate the migration of NSCs towards the ischaemic lesion. The therapeutic potential of such SDF-1 enhanced hDPSCs in the context of stroke could be a subject worthy to investigate.

Prior studies with hDPSCs already demonstrated the capacity of these stem cells to promote survival of sensory and dopaminergic neurons and to inhibit neuronal cell death after spinal cord injury [39, 41, 65, 66]. Here, the capacity of hDPSCs to exert neuroprotective effects in stroke is of interest. To evaluate the neuroprotective capacity of hDPSCs *in vitro*, an OGD survival assay is developed since OGD is a hallmark pathological condition in ischaemic stroke. This assay includes induction of OGD in pCNs, followed by exposure to the CM of hDPSCs. However, the OGD survival assay has to be optimized in order to obtain accurate and consistent results. Firstly, a pCN culture needed to be

established. The morphological properties of pCN cultures at varying cell densities were evaluated. At densities of 6 x 10^4 cells/cm^2 and higher, the cells formed aggregates and developed neurites that extended to the periphery of the aggregates. From densities of 1.2 x 10^5 cells/cm^2 the formation of strong neuronal connections between the aggregates was observed. Secondly, the use of the AlamarBlue® viability assay in pCNs was validated. As expected, a linear correlation was observed between cell density and FI. Furthermore, with increasing incubation time of the AlamarBlue dye, the fluorescence signal was more intense for a given cell density. In order to obtain optimal results with the OGD survival assay, it is suggested to use a cell density and incubation time whereby the highest FI can be measured without acquiring saturation of the signal intensity. This ensures the highest sensitivity is obtained for the detection of the metabolic activity in the pCNs. Taken together, a stable pCN culture could be established. When using pCN cultures for the OGD assay, it is recommended to use a cell density of at least 1.2 x 10^5 cells/cm^2 and an AlamarBlue® incubation time of 6h, since with these parameters optimal results were obtained. Moreover, it is noteworthy to mention that the metabolic activity is dependent on the culture period of the pCNs. In rat pCNs a maximal metabolic activity is observed between 14 and 20 days *in vitro* [80]. Thus, pCN cultures of the same age should be used for comparison to prevent this experimental bias.

Finally, the OGD exposure time had to be optimized. The pCNs were exposed to OGD for varying periods and consequently incubated in control medium. Standard pCN medium and α-MEM + 0.1% were both used for optimization, since the CM of hDPSCs was also produced in these media. In both the condition with standard pCN medium and α-MEM, the metabolic activity seemed to decrease with increasing OGD time, with the exception of the 3h OGD in the α-MEM condition measured immediately after OGD. Here, the metabolic activity seemed to be strongly increased. It could be speculated that exposure to α-MEM after 3h of OGD puts additional stress on the cells, since α-MEM is a nutrient poor medium compared to standard pCN medium, thereby driving the cells to increase their metabolic activity in an attempt to survive. When the metabolic activity was measured 24h later, the metabolic activity was drastically reduced, indicating a reduction in cell viability. This phenomenon was not observed after 1h OGD. A possible explanation might be that in the 1h OGD, not enough stress is induced to affect the viability of the cells. However, this could not be confirmed, since no positive control was included in this experiment. After 24h of OGD, no sign of metabolic activity was observed, indicating a complete reduction in cell viability. Taken together, no definite conclusions can be drawn from this experiment. The results strongly suggest that OGD induces cell death with increasing OGD time, but more elaborate investigation is necessary to determine an OGD time at which a significant reduction in cell viability is observed without completely killing the total pCN population. A similar study, conducted by the research group of White *et al.* showed that 24h of OGD in rat pCNs resulted in a 25% reduction in cell viability and 48h of OGD in a reduction of 85% [80]. In order to evaluate the capacity of hDPSCs to exert neuroprotective effects, the OGD survival assay has to be further optimized. It is strongly suggested to make use of higher cell densities in the following experiments. Here, only 6 x 10^4 cells/cm^2 were used, while the complementary experiments indicate that a minimal cell density of 1.2 x 10^5 cells/cm^2 should be used. This should increase the sensitivity of the assay and reduce the variability. In addition, a positive control should be included to be able to determine the percentage of viability reduction.

Supplementary to the AlamarBlue® viability assay, a flow cytometric annexin V/PI apoptosis assay was performed to investigate if actual cell death was present in the pCN culture. Low percentages of cell death were observed in all conditions, including the control condition. These dead cells were all positive for PI, indicating these cells underwent necrosis. No increase in cell death could be observed after 1h and 3h of OGD compared to the control condition. However, this is not in accordance with a similar study that used the annexin V/PI assay to evaluate the survival of rat pCNs after OGD [81]. In this study, increased cell death was present after 90 min. of OGD. Moreover, many apoptotic cells (annexin V positive) could be observed, whereas in our experiment no apoptotic cells could be observed. Albeit, the presence of apoptosis is expected since OGD leads to the initiation of a cascade of deleterious events including membrane depolarization, mitochondrial failure, ROS accumulation and activation of proteolytic enzymes, which induce apoptosis [5]. Therefore, it is suggested to repeat the annexin V/PI to evaluate if these discrepancies are due to experimental error.

Human DPSCs have been shown to provide axon guidance *in ovo* and stimulate neurite outgrowth in a rat model of spinal cord injury [39, 40]. Moreover, the chemoattractant guidance of the axons was mediated via the SDF-1/CXCR4 pathway. In this study, it was attempted to reconstitute these findings in pCNs. A neurite analysis was performed after pCNs were exposed to the CM of hDPSCs. No significant difference in average neurite length could be observed between the pCNs exposed to the control medium and the CM of the hDPSCs after 96 hours in culture. Moreover, the CM of the hDPSCs had no significant effect on the amount of neurites per cell. Thus, the beneficial effect of hDPSCs on neurite outgrowth in neurons observed in previous studies could not be reconstituted in pCNs in this *in vitro* setting. The performed experiment could be repeated using higher cell densities, since in this experiment a suboptimal cell density was used (3×10^4 cells/cm^2). As previously described, the pCN cultures only started to develop pronounced neurite outgrowth when cell densities of at least 6×10^4 cell/cm^2 were used. Thereby, repeating the experiment with a higher cell density should result in a more accurate analysis. Additionally, if beneficial effects of hDPSCs on neurite outgrowth in pCNs were to be obtained, the importance of the SDF-1/CXCR4 axis in this effect could be examined by inhibiting this pathway with antibodies directed against SDF-1.

The use of iPSC in regenerative medicine is making progress. Transplantation of iPSC-derived neurospheres in a mouse model of spinal cord injury showed that the cells migrate towards the lesion, differentiate into neurons, astrocytes and oligodendrocytes *in vivo* and improve motor function [50]. Furthermore, human iPSC-derived neurons were able to promote functional recovery after transplantation in stroke-damaged rats [51, 52]. These findings demonstrate the therapeutic potential of iPSCs in pathological conditions of the CNS. In order to investigate these pluripotent stem cells in our lab, an iPSC culture has to be established. However, prior to establishing an iPSC culture a feeder cell-dependent H9 ESCs culture was introduced in the lab, since this is considered to be the golden standard of pluripotent stem cell culture. Maintenance of a proper pluripotent stem cell culture is labour-intensive and requires a certain amount of expertise. Therefore, introduction of an H9 hESC culture allowed to gain experience with pluripotent stem cell culture, establish protocols for immunocytochemical and ultrastructural analysis and allows comparison of the iPSC culture with an already established culture of pluripotent stem cells. Immunocytochemical analysis

of the H9 ESCs showed expression of hallmark pluripotency markers. The master transcription factors Nanog, Oct-4 and Sox2 are essential for the maintenance of pluripotency in these cells [82-84]. They bind to enhancer elements which regulate the activity of genes that control the pluripotent state and thereby are responsible for the induction of the pluripotent gene expression profile. The function of tra-1-60 and tra-1-81 remains to be elucidated, but these markers are widely used for identification of human cancers and ESC lines [85]. Ultrastructural analysis of the H9 hESC colonies showed that the cells were tightly packed and often made cell-cell contact. Furthermore, the cells contained low amounts of cell organelles such as mitochondria, endoplasmic reticulum and Golgi complexes, indicating an undifferentiated state. Morphologically, the H9 ESC cultures displayed characteristics of a standard pluripotent stem cell culture [86]. Though, it has to be emphasized that consequent removal of colonies that develop signs of differentiation, is essential to preserve a healthy culture. Taken together, these findings suggests that an undifferentiated, pluripotent stem cell culture was established. Further characterization of the H9 ESCs could include embryoid body formation and teratoma formation to evaluate if cell derivatives of the three germ layers can be generated.

5 Conclusion

Currently, there is no cure for stroke patients and existing treatment strategies are unable to sufficiently improve the functional outcome following stroke. However, cell-based therapy is considered a promising approach to minimize neurological damage and enhance functional recovery. In this study, the goal was to identify neuroprotective and neuroregenerative effects of hDPSCs *in vitro* and their potential underlying mechanisms. Providing stressed neurons with neurotrophic and anti-apoptotic signals could allow them to survive the harsh conditions in the acute phase of stroke, thereby limiting stroke severity and neurological damage. Furthermore, stimulating neuroregeneration after stroke could result in enhanced functional recovery. Investigating both the short- and long-term beneficial effects of hDPSCs on the disease outcome in stroke is essential for a profound understanding of the therapeutic potential.

To evaluate the capacity of hDPSCs to promote neurogenesis *in vitro*, NSCs are the most relevant cell type to use since they give rise to the neuronal cells in the brain. Therefore, a stable NSC culture needed to be established. The isolated NSCs were morphologically and phenotypically characterized. However, it is recommended to perform additional characterization experiments to verify the purity of the acquired NSC culture. These should include validation of the differentiation capacity towards neurons, astrocytes and oligodendrocyte. The obtained NSC culture can be used to evaluate the potential of the secretome of hDPSCs to stimulate directed migration of NSCs and to induce differentiation of NSCs towards neuronal cell lineages. Furthermore, the interaction between hDPSCs and NSCs could be used to study the role of the CXCR4/SDF-1 axis in this migration process.

To evaluate the neuroprotective capacity of hDPSCs *in vitro*, an OGD survival assay was developed since OGD is a hallmark pathological condition in ischaemic stroke. Therefore, a pCN culture had to be established first. Consequently, the AlamarBlue® was validated in a pCN culture. The obtained results indicated that the use of a cell density of at least 1.2×10^5 cell/cm^2 and an incubation time of 6h is recommended to perform the OGD survival assay. A first attempt was undertaken to optimize the OGD exposure time. The findings suggested that cell viability decreased with increasing OGD time. However, further investigation is necessary to determine an OGD time at which a significant reduction in cell viability can be achieved in a fraction of pCNs. Once the OGD survival assay is optimized, it can be assessed whether the secretome of hDPSCs is able to enhance survival of pCNs which are exposed to OGD.

Additionally, a H9 hESC culture was introduced in the lab to gain experience with pluripotent stem cell culture to allow comparison of the future iPSC culture with an already established culture of pluripotent stem cells.

In conclusion, the capacity of hDPSCs to exert neuroprotective and neuroregenerative effect *in vitro* could not be investigated yet. However, preceding experiments were performed which were necessary to provide established cell cultures and knowledge about the optimal conditions for future assays. More elaborate research will grant information about the neuroprotective and neuroregenerative capacity of hDPSCs and reveal insight in the therapeutic potential of hDPSCs in ischaemic stroke.

References

1. Feigin VL, Forouzanfar MH, Krishnamurthi R, et al. Global and regional burden of stroke during 1990-2010: findings from the Global Burden of Disease Study 2010. Lancet. 2014;383(9913):245-54.
2. Donnan GA, Fisher M, Macleod M, et al. Stroke. Lancet. 2008;371(9624):1612-23.
3. Maas MB. Ischemic stroke: Pathophysiology and principles of localization. Neurology board review manual; 2009. p. 1-16.
4. Durukan A, Tatlisumak T. Acute ischemic stroke: overview of major experimental rodent models, pathophysiology, and therapy of focal cerebral ischemia. Pharmacology, biochemistry, and behavior. 2007;87(1):179-97.
5. Schmidt A, Minnerup J, Kleinschnitz C. Emerging neuroprotective drugs for the treatment of acute ischaemic stroke. Expert opinion on emerging drugs. 2013;18(2):109-20.
6. Sutherland BA, Minnerup J, Balami JS, et al. Neuroprotection for ischaemic stroke: translation from the bench to the bedside. International journal of stroke : official journal of the International Stroke Society. 2012;7(5):407-18.
7. Bandera E, Botteri M, Minelli C, et al. Cerebral blood flow threshold of ischemic penumbra and infarct core in acute ischemic stroke: a systematic review. Stroke; a journal of cerebral circulation. 2006;37(5):1334-9.
8. Simard JM, Kent TA, Chen M, et al. Brain oedema in focal ischaemia: molecular pathophysiology and theoretical implications. The Lancet Neurology. 2007;6(3):258-68.
9. Huang J, Upadhyay UM, Tamargo RJ. Inflammation in stroke and focal cerebral ischemia. Surgical neurology. 2006;66(3):232-45.
10. Magnus T, Wiendl H, Kleinschnitz C. Immune mechanisms of stroke. Current opinion in neurology. 2012;25(3):334-40.
11. Moretti A, Ferrari F, Villa RF. Neuroprotection for ischaemic stroke: Current status and challenges. Pharmacology & therapeutics. 2015;146C:23-34.
12. Molina CA. Reperfusion therapies for acute ischemic stroke: current pharmacological and mechanical approaches. Stroke; a journal of cerebral circulation. 2011;42(1 Suppl):S16-9.
13. Lees KR, Bluhmki E, von Kummer R, et al. Time to treatment with intravenous alteplase and outcome in stroke: an updated pooled analysis of ECASS, ATLANTIS, NINDS, and EPITHET trials. Lancet. 2010;375(9727):1695-703.
14. Ciccone A, Valvassori L, Nichelatti M, et al. Endovascular treatment for acute ischemic stroke. The New England journal of medicine. 2013;368(10):904-13.
15. Ginsberg MD. Neuroprotection for ischemic stroke: past, present and future. Neuropharmacology. 2008;55(3):363-89.
16. Mergenthaler P, Dirnagl U, Meisel A. Pathophysiology of stroke: lessons from animal models. Metabolic brain disease. 2004;19(3-4):151-67.
17. Zhang ZG, Chopp M. Neurorestorative therapies for stroke: underlying mechanisms and translation to the clinic. The Lancet Neurology. 2009;8(5):491-500.
18. Hermann DM, Chopp M. Promoting brain remodelling and plasticity for stroke recovery: therapeutic promise and potential pitfalls of clinical translation. The Lancet Neurology. 2012;11(4):369-80.

19. Lakshmipathy U, Verfaillie C. Stem cell plasticity. Blood reviews. 2005;19(1):29-38.
20. Martens W, Bronckaers A, Politis C, et al. Dental stem cells and their promising role in neural regeneration: an update. Clinical oral investigations. 2013;17(9):1969-83.
21. Dominici M, Le Blanc K, Mueller I, et al. Minimal criteria for defining multipotent mesenchymal stromal cells. The International Society for Cellular Therapy position statement. Cytotherapy. 2006;8(4):315-7.
22. Uccelli A, Moretta L, Pistoia V. Mesenchymal stem cells in health and disease. Nature reviews Immunology. 2008;8(9):726-36.
23. Giordano A, Galderisi U, Marino IR. From the laboratory bench to the patient's bedside: an update on clinical trials with mesenchymal stem cells. Journal of cellular physiology. 2007;211(1):27-35.
24. Gronthos S, Mankani M, Brahim J, et al. Postnatal human dental pulp stem cells (DPSCs) in vitro and in vivo. Proceedings of the National Academy of Sciences of the United States of America. 2000;97(25):13625-30.
25. Miura M, Gronthos S, Zhao M, et al. SHED: stem cells from human exfoliated deciduous teeth. Proceedings of the National Academy of Sciences of the United States of America. 2003;100(10):5807-12.
26. Seo BM, Miura M, Gronthos S, et al. Investigation of multipotent postnatal stem cells from human periodontal ligament. Lancet. 2004;364(9429):149-55.
27. Sonoyama W, Liu Y, Fang D, et al. Mesenchymal stem cell-mediated functional tooth regeneration in swine. PloS one. 2006;1:e79.
28. Morsczeck C, Gotz W, Schierholz J, et al. Isolation of precursor cells (PCs) from human dental follicle of wisdom teeth. Matrix biology : journal of the International Society for Matrix Biology. 2005;24(2):155-65.
29. Gronthos S, Brahim J, Li W, et al. Stem cell properties of human dental pulp stem cells. Journal of dental research. 2002;81(8):531-5.
30. Alge DL, Zhou D, Adams LL, et al. Donor-matched comparison of dental pulp stem cells and bone marrow-derived mesenchymal stem cells in a rat model. Journal of tissue engineering and regenerative medicine. 2010;4(1):73-81.
31. Huang GT, Gronthos S, Shi S. Mesenchymal stem cells derived from dental tissues vs. those from other sources: their biology and role in regenerative medicine. Journal of dental research. 2009;88(9):792-806.
32. Struys T, Moreels M, Martens W, et al. Ultrastructural and immunocytochemical analysis of multilineage differentiated human dental pulp- and umbilical cord-derived mesenchymal stem cells. Cells, tissues, organs. 2011;193(6):366-78.
33. Kiraly M, Kadar K, Horvathy DB, et al. Integration of neuronally predifferentiated human dental pulp stem cells into rat brain in vivo. Neurochemistry international. 2011;59(3):371-81.
34. Paino F, Ricci G, De Rosa A, et al. Ecto-mesenchymal stem cells from dental pulp are committed to differentiate into active melanocytes. European cells & materials. 2010;20:295-305.

35. Huang GT, Yamaza T, Shea LD, et al. Stem/progenitor cell-mediated de novo regeneration of dental pulp with newly deposited continuous layer of dentin in an in vivo model. Tissue engineering Part A. 2010;16(2):605-15.
36. Gandia C, Arminan A, Garcia-Verdugo JM, et al. Human dental pulp stem cells improve left ventricular function, induce angiogenesis, and reduce infarct size in rats with acute myocardial infarction. Stem cells. 2008;26(3):638-45.
37. Nakashima M, Iohara K, Sugiyama M. Human dental pulp stem cells with highly angiogenic and neurogenic potential for possible use in pulp regeneration. Cytokine & growth factor reviews. 2009;20(5-6):435-40.
38. Leong WK, Henshall TL, Arthur A, et al. Human adult dental pulp stem cells enhance poststroke functional recovery through non-neural replacement mechanisms. Stem cells translational medicine. 2012;1(3):177-87.
39. Sakai K, Yamamoto A, Matsubara K, et al. Human dental pulp-derived stem cells promote locomotor recovery after complete transection of the rat spinal cord by multiple neuro-regenerative mechanisms. The Journal of clinical investigation. 2012;122(1):80-90.
40. Arthur A, Shi S, Zannettino AC, et al. Implanted adult human dental pulp stem cells induce endogenous axon guidance. Stem cells. 2009;27(9):2229-37.
41. Nosrat IV, Smith CA, Mullally P, et al. Dental pulp cells provide neurotrophic support for dopaminergic neurons and differentiate into neurons in vitro; implications for tissue engineering and repair in the nervous system. The European journal of neuroscience. 2004;19(9):2388-98.
42. Perry BC, Zhou D, Wu X, et al. Collection, cryopreservation, and characterization of human dental pulp-derived mesenchymal stem cells for banking and clinical use. Tissue engineering Part C, Methods. 2008;14(2):149-56.
43. Thomson JA, Itskovitz-Eldor J, Shapiro SS, et al. Embryonic stem cell lines derived from human blastocysts. Science. 1998;282(5391):1145-7.
44. Muller FJ, Laurent LC, Kostka D, et al. Regulatory networks define phenotypic classes of human stem cell lines. Nature. 2008;455(7211):401-5.
45. Takahashi K, Yamanaka S. Induction of pluripotent stem cells from mouse embryonic and adult fibroblast cultures by defined factors. Cell. 2006;126(4):663-76.
46. Takahashi K, Tanabe K, Ohnuki M, et al. Induction of pluripotent stem cells from adult human fibroblasts by defined factors. Cell. 2007;131(5):861-72.
47. Yu J, Vodyanik MA, Smuga-Otto K, et al. Induced pluripotent stem cell lines derived from human somatic cells. Science. 2007;318(5858):1917-20.
48. Kaji K, Norrby K, Paca A, et al. Virus-free induction of pluripotency and subsequent excision of reprogramming factors. Nature. 2009;458(7239):771-5.
49. Kriks S, Shim JW, Piao J, et al. Dopamine neurons derived from human ES cells efficiently engraft in animal models of Parkinson's disease. Nature. 2011;480(7378):547-51.
50. Nori S, Okada Y, Yasuda A, et al. Grafted human-induced pluripotent stem-cell-derived neurospheres promote motor functional recovery after spinal cord injury in mice. Proceedings of the National Academy of Sciences of the United States of America. 2011;108(40):16825-30.

51. Oki K, Tatarishvili J, Wood J, et al. Human-induced pluripotent stem cells form functional neurons and improve recovery after grafting in stroke-damaged brain. Stem cells. 2012;30(6):1120-33.
52. Tornero D, Wattananit S, Gronning Madsen M, et al. Human induced pluripotent stem cell-derived cortical neurons integrate in stroke-injured cortex and improve functional recovery. Brain : a journal of neurology. 2013;136(Pt 12):3561-77.
53. Devine MJ, Ryten M, Vodicka P, et al. Parkinson's disease induced pluripotent stem cells with triplication of the alpha-synuclein locus. Nature communications. 2011;2:440.
54. Israel MA, Yuan SH, Bardy C, et al. Probing sporadic and familial Alzheimer's disease using induced pluripotent stem cells. Nature. 2012;482(7384):216-20.
55. Brennand KJ, Simone A, Jou J, et al. Modelling schizophrenia using human induced pluripotent stem cells. Nature. 2011;473(7346):221-5.
56. Lees JS, Sena ES, Egan KJ, et al. Stem cell-based therapy for experimental stroke: a systematic review and meta-analysis. International journal of stroke : official journal of the International Stroke Society. 2012;7(7):582-8.
57. Jeong H, Yim HW, Cho YS, et al. Efficacy and safety of stem cell therapies for patients with stroke: a systematic review and single arm meta-analysis. International journal of stem cells. 2014;7(2):63-9.
58. Hilkens P, Gervois P, Fanton Y, et al. Effect of isolation methodology on stem cell properties and multilineage differentiation potential of human dental pulp stem cells. Cell and tissue research. 2013;353(1):65-78.
59. Mead B, Logan A, Berry M, et al. Paracrine-mediated neuroprotection and neuritogenesis of axotomised retinal ganglion cells by human dental pulp stem cells: comparison with human bone marrow and adipose-derived mesenchymal stem cells. PloS one. 2014;9(10):e109305.
60. Song M, Jue SS, Cho YA, et al. Comparison of the effects of human dental pulp stem cells and human bone marrow-derived mesenchymal stem cells on ischemic human astrocytes in vitro. Journal of neuroscience research. 2015;93(6):973-83.
61. Zhang Y, Wang D, Cao K, et al. Rat induced pluripotent stem cells protect H9C2 cells from cellular senescence via a paracrine mechanism. Cardiology. 2014;128(1):43-50.
62. Espuny-Camacho I, Michelsen KA, Gall D, et al. Pyramidal neurons derived from human pluripotent stem cells integrate efficiently into mouse brain circuits in vivo. Neuron. 2013;77(3):440-56.
63. Gervois P, Struys T, Hilkens P, et al. Neurogenic Maturation of Human Dental Pulp Stem Cells Following Neurosphere Generation Induces Morphological and Electrophysiological Characteristics of Functional Neurons. Stem cells and development. 2014.
64. Fang CZ, Yang YJ, Wang QH, et al. Intraventricular injection of human dental pulp stem cells improves hypoxic-ischemic brain damage in neonatal rats. PloS one. 2013;8(6):e66748.
65. de Almeida FM, Marques SA, Ramalho Bdos S, et al. Human dental pulp cells: a new source of cell therapy in a mouse model of compressive spinal cord injury. Journal of neurotrauma. 2011;28(9):1939-49.

66. Apel C, Forlenza OV, de Paula VJ, et al. The neuroprotective effect of dental pulp cells in models of Alzheimer's and Parkinson's disease. Journal of neural transmission. 2009;116(1):71-8.
67. Huang AH, Snyder BR, Cheng PH, et al. Putative dental pulp-derived stem/stromal cells promote proliferation and differentiation of endogenous neural cells in the hippocampus of mice. Stem cells. 2008;26(10):2654-63.
68. Martens W, Wolfs E, Struys T, et al. Expression pattern of basal markers in human dental pulp stem cells and tissue. Cells, tissues, organs. 2012;196(6):490-500.
69. Reekmans KP, Praet J, De Vocht N, et al. Clinical potential of intravenous neural stem cell delivery for treatment of neuroinflammatory disease in mice? Cell transplantation. 2011;20(6):851-69.
70. Glaser T, Pollard SM, Smith A, et al. Tripotential differentiation of adherently expandable neural stem (NS) cells. PloS one. 2007;2(3):e298.
71. Conti L, Pollard SM, Gorba T, et al. Niche-independent symmetrical self-renewal of a mammalian tissue stem cell. PLoS Biol. 2005;3(9):e283.
72. Thored P, Arvidsson A, Cacci E, et al. Persistent production of neurons from adult brain stem cells during recovery after stroke. Stem cells. 2006;24(3):739-47.
73. Yu X, Chen D, Zhang Y, et al. Overexpression of CXCR4 in mesenchymal stem cells promotes migration, neuroprotection and angiogenesis in a rat model of stroke. J Neurol Sci. 2012;316(1-2):141-9.
74. Iohara K, Zheng L, Wake H, et al. A novel stem cell source for vasculogenesis in ischemia: subfraction of side population cells from dental pulp. Stem cells. 2008;26(9):2408-18.
75. Kucia M, Reca R, Miekus K, et al. Trafficking of normal stem cells and metastasis of cancer stem cells involve similar mechanisms: pivotal role of the SDF-1-CXCR4 axis. Stem cells. 2005;23(7):879-94.
76. Janowska-Wieczorek A, Marquez LA, Dobrowsky A, et al. Differential MMP and TIMP production by human marrow and peripheral blood CD34(+) cells in response to chemokines. Exp Hematol. 2000;28(11):1274-85.
77. Imitola J, Raddassi K, Park KI, et al. Directed migration of neural stem cells to sites of CNS injury by the stromal cell-derived factor 1alpha/CXC chemokine receptor 4 pathway. Proceedings of the National Academy of Sciences of the United States of America. 2004;101(52):18117-22.
78. Zhang M, Mal N, Kiedrowski M, et al. SDF-1 expression by mesenchymal stem cells results in trophic support of cardiac myocytes after myocardial infarction. FASEB J. 2007;21(12):3197-207.
79. Kortesidis A, Zannettino A, Isenmann S, et al. Stromal-derived factor-1 promotes the growth, survival, and development of human bone marrow stromal stem cells. Blood. 2005;105(10):3793-801.
80. White MJ, DiCaprio MJ, Greenberg DA. Assessment of neuronal viability with Alamar blue in cortical and granule cell cultures. Journal of neuroscience methods. 1996;70(2):195-200.

81. Liu Y, Zhang Y, Lin L, et al. Effects of bone marrow-derived mesenchymal stem cells on the axonal outgrowth through activation of PI3K/AKT signaling in primary cortical neurons followed oxygen-glucose deprivation injury. PloS one. 2013;8(11):e78514.
82. Chambers I, Colby D, Robertson M, et al. Functional expression cloning of Nanog, a pluripotency sustaining factor in embryonic stem cells. Cell. 2003;113(5):643-55.
83. Avilion AA, Nicolis SK, Pevny LH, et al. Multipotent cell lineages in early mouse development depend on SOX2 function. Genes Dev. 2003;17(1):126-40.
84. Nichols J, Zevnik B, Anastassiadis K, et al. Formation of pluripotent stem cells in the mammalian embryo depends on the POU transcription factor Oct4. Cell. 1998;95(3):379-91.
85. Schopperle WM, DeWolf WC. The TRA-1-60 and TRA-1-81 human pluripotent stem cell markers are expressed on podocalyxin in embryonal carcinoma. Stem cells. 2007;25(3):723-30.
86. Schwartz PH, Brick DJ, Nethercott HE, et al. Traditional human embryonic stem cell culture. Methods Mol Biol. 2011;767:107-23.

Supplementary information

S1 Induction of cell death in pCNs by glutamate excitotoxicity

In analogy with the OGD survival assay, the induction of cell death by glutamate excitotoxicity was investigated *(fig. S1).*

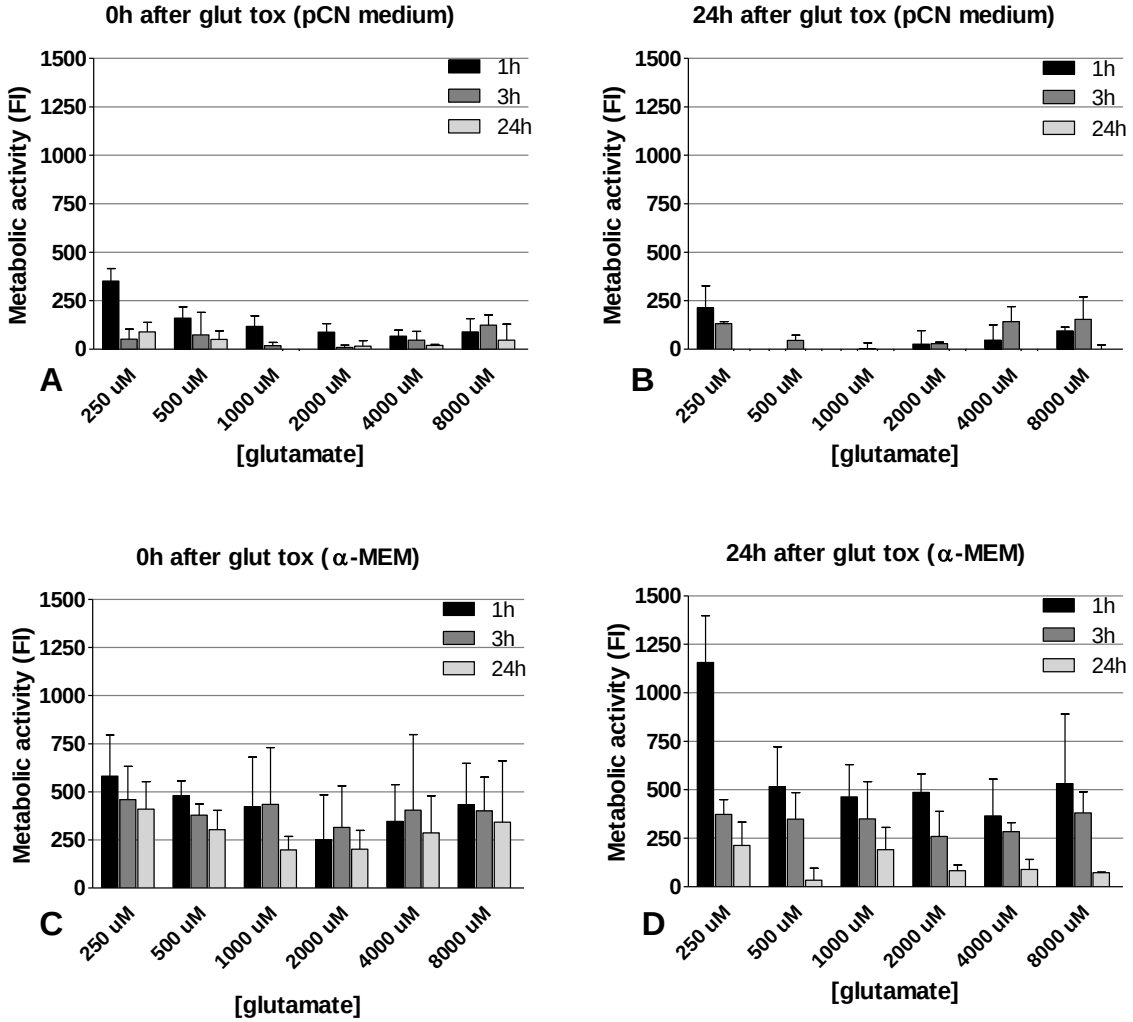

Figure S1: Induction of cell death in pCNs by glutamate excitotoxicity.
In analogy with the OGD survival assay, the induction of cell death by glutamate excitotoxicity was investigated. The pCN were exposed to varying concentrations of glutamate (250 µM – 8 mM) for 1h, 3h and 24h. Consequently, the metabolic activity was measured immediately after glutamate exposure and 24h later, with the AlamarBlue® assay. **(A-B)** In the condition with standard pCN medium, exposure to 250 µM glutamate for 1h resulted in a FI value of 351.3 (SD = 65.6). When the pCNs were exposed to increasing concentrations of glutamate for 1h, the metabolic activity appeared to reduce. Exposure to glutamate for 3h and 24h seemed to reduce the metabolic activity drastically. When the metabolic activity was measured 24h later, even lower values are observed. **(C-D)** In the condition with α-MEM, higher values of FI are observed compared to the condition with standard pCN medium. Exposure to 250 µM glutamate for 1h resulted in a FI value of 582.3 (SD = 213.4). With increasing exposure time and increasing glutamate concentrations the metabolic activity also seemed to decline. When measured 24h later, the metabolic activity in the 250 µM condition was higher compared with the value measured immediately after 1h of exposure. With increasing concentrations and exposure time the metabolic activity appeared to decline.

Auteursrechtelijke overeenkomst

Ik/wij verlenen het wereldwijde auteursrecht voor de ingediende eindverhandeling:
Neuroprotective and neural reparative capacity of human dental pulp stem cells: identification of the CXCR4/SDF-1 migratory pathway

Richting: **master in de biomedische wetenschappen-klinische moleculaire wetenschappen**
Jaar: **2015**

in alle mogelijke mediaformaten, - bestaande en in de toekomst te ontwikkelen - , aan de Universiteit Hasselt.

Niet tegenstaand deze toekenning van het auteursrecht aan de Universiteit Hasselt behoud ik als auteur het recht om de eindverhandeling, - in zijn geheel of gedeeltelijk -, vrij te reproduceren, (her)publiceren of distribueren zonder de toelating te moeten verkrijgen van de Universiteit Hasselt.

Ik bevestig dat de eindverhandeling mijn origineel werk is, en dat ik het recht heb om de rechten te verlenen die in deze overeenkomst worden beschreven. Ik verklaar tevens dat de eindverhandeling, naar mijn weten, het auteursrecht van anderen niet overtreedt.

Ik verklaar tevens dat ik voor het materiaal in de eindverhandeling dat beschermd wordt door het auteursrecht, de nodige toelatingen heb verkregen zodat ik deze ook aan de Universiteit Hasselt kan overdragen en dat dit duidelijk in de tekst en inhoud van de eindverhandeling werd genotificeerd.

Universiteit Hasselt zal mij als auteur(s) van de eindverhandeling identificeren en zal geen wijzigingen aanbrengen aan de eindverhandeling, uitgezonderd deze toegelaten door deze overeenkomst.

Voor akkoord,

Dillen, Yörg

Datum: **9/06/2015**